

# Phenomenological Analysis of $B \rightarrow PP$ Decays with QCD Factorization \*

Dongsheng Du,<sup>1,2</sup> Haijun Gong,<sup>2</sup> Junfeng Sun,<sup>2</sup> Deshan Yang,<sup>2</sup> and Guohuai Zhu<sup>2</sup>

1. *CCAST (World Laboratory), P.O.Box 8730, Beijing 100080, China*

2. *Institute of High Energy Physics, Chinese Academy of Sciences,*

*P.O.Box 918(4), Beijing 100039, China* † ‡

(October 22, 2018)

## Abstract

In this paper, we study nonleptonic charmless  $B$  decays to two light pseudoscalar mesons within the frame of QCD factorization, including the contributions from the chirally enhanced power corrections and weak annihilation. Predictions for the CP-averaged branching ratios and CP-violating asymmetries are given. Within the reasonable range of the parameters, we find that our predictions for the branching ratios of  $B \rightarrow PP$  are consistent with the present experimental data. But because of the logarithmic divergences at the endpoints in the hard spectator scatterings and weak annihilation, there are still large uncertainties in these predictions.

**PACS numbers 13.25.Hw 12.38.Bx**

---

\*Supported in part by National Natural Science Foundation of China.

†Mailing address

‡Email:duds@mail.ihep.ac.cn,

gonghj@mail.ihep.ac.cn,

sunjf@mail.ihep.ac.cn,

yangds@mail.ihep.ac.cn, zhugh@mail.ihep.ac.cn

## I. INTRODUCTION

In the standard model (SM), CP violation and quark mixing are closely related to each other. The unitarity of the Cabibbo-Kobayashi-Maskawa (CKM) matrix implies various relations among its elements. The most commonly studied is the “unitarity triangle”:  $V_{ud}V_{ub}^* + V_{cd}V_{cb}^* + V_{td}V_{tb}^* = 0$ . The study of  $B$  meson decays is mainly to make enough independent measurements for the sides and angles ( $\alpha$ ,  $\beta$  and  $\gamma$ ) of this unitarity triangle. For example, in principle,  $\sin 2\beta$  can be determined by measurements of the time dependent CP asymmetries of the decay  $\bar{B}_d^0 \rightarrow J/\Psi K_S$  and other related modes with an uncertainty less than 1%. On the other hand, we can also extract or give a constraint for the angle  $\alpha$  from the decay  $B \rightarrow \pi\pi$ , and the angle  $\gamma$  from  $B \rightarrow \pi\pi$  and  $\pi K$ . Compared with determination of  $\sin 2\beta$ , the extractions of  $\alpha$  and  $\gamma$  from exclusively non-leptonic charmless  $B$  decays suffer from significant theoretical uncertainties for the strong interactions.

Experimentally, many  $B$  experiment projects have been running (CLEO, BaBar, Belle, etc.), or will run in forthcoming years (BTeV, CERN LHCb, DESY HeraB, etc.). Several collaborations have reported their latest results recently [1–3], and more  $B$  decay channels will be measured with great precision soon. Among these decay channels, quite a few are nonleptonic charmless two-body modes, such as  $B \rightarrow \pi K$ ,  $\pi\pi$ ,  $K\eta'$ , etc. With the accumulation of the experimental data, the theorists are urged to gain a deep insight into rare hadronic  $B$  meson decays, and to reduce the theoretical errors in determining the CKM parameters from the experimental data.

Theoretically, the nonleptonic charmless two-body  $B$  decays have been widely discussed and carefully studied in the framework of the effective Hamiltonian and factorization hypothesis. The effective Hamiltonian is obtained by operator product expansion (OPE) and the renormalization group (RG) method, and generally expressed as the product of the Wilson coefficients and the effective operators, in forms of the four-quarks and magnetic moment operators. The Wilson coefficients can be calculated reliably by the perturbation theory. In the SM, they have been evaluated to next-to-leading order [4]. Thus, the main task for us is to compute the hadronic matrix elements of the effective operators. However, the complexity of QCD dynamics does not allow us to compute them directly from first principles. Generally, we resort to the factorization approximation [5], ignoring the soft interactions between the ejected meson and recoiling system. Under this approximation, the hadronic matrix element of the effective operator can be parameterized into the product of the meson decay constant and the meson-meson transition form factor. A comprehensive analysis for nonleptonic charmless two-body  $B$  decays based on the naive factorization and/or generalized factorization was done in the past decade, and achieved great success.

The factorization approximation does hold in the limit that the soft interactions in the initial and final states can be ignored. It seems that the argument of color-transparency can give reasonable support to the above limit [6]. Because the  $b$  quark is heavy, the quarks from  $b$  quark decay move so fast that a pair of quark and antiquark in a small color-singlet object decouples from the soft interactions. But for the case of naive factorization the shortcomings are obvious. First, the renormalization scheme and scale dependence in the hadronic matrix elements of the effective operators are apparently missed. Then the full decay amplitude predicted by the Bauer-Stech-Wirbel (BSW) model remains dependent on the renormalization scheme and scale, which are mainly from the Wilson coefficients. In

recent years, many researchers have generalized the naive factorization scheme and made remarkable progress, such as the scheme and scale independent effective Wilson coefficients, effective color number, which is introduced to compensate the “non-factorizable” contributions, etc. [7]. Furthermore, some progress in nonperturbative methods, such as lattice QCD, QCD sum rules etc. [8–10], allow us to compute many non-perturbative parameters in  $B$  decays, such as the meson decay constants and meson-meson transition form factors. Every improvement allows us to have a closer look at the  $B$  nonleptonic decays. In [11,12], the authors gave a comprehensive and detailed analysis for the nonleptonic two-body charmless  $B$  decays within the frame of the generalized factorization.

Two year ago, Beneke, Buchalla, Neubert, and Sachrajda (BBNS) gave a QCD factorization formula in the heavy quark limit for the decays  $B \rightarrow \pi\pi$  [13]. They pointed out that the radiative corrections from hard gluon exchange can be systematically calculated by use of the perturbative QCD method in the heavy quark limit, i.e., neglecting the power contributions of  $\Lambda_{QCD}/m_b$ . This factorization formula can be justified in the case that the ejected meson from the  $b$  quark decay is a light meson or an onium, no matter whether the other recoiling meson which absorbs the spectator quark in the  $B$  meson is light or heavy. But for the case that the ejected meson is in an extremely asymmetric configuration, such as a  $D$  meson, this factorization formula does not hold. The contributions from hard scattering with the spectator quark in the  $B$  meson are also involved in their formula. This kind of contribution cannot be contained in the naive factorization, but it appears at the order of  $\alpha_s$ . So the naive factorization can be recovered if one neglects the radiative corrections and suppressed power  $\Lambda_{QCD}/m_b$  contributions in the QCD factorization. The non-factorizable contributions in the naive factorization can be calculated perturbatively, so we do not need a phenomenological parameter  $N_c^{eff}$  to compensate the non-factorizable effects. Moreover, because the  $b$  quark mass is not very large in reality, the potential power corrections, in particular, the chirally enhanced corrections, will play an important role in  $B \rightarrow PP$  [14–16]. So the twist-3 light-cone wave function of the light pseudoscalar must be taken into account. Unfortunately, QCD factorization breaks down at twist-3 level. There is a logarithmic divergence in the hard spectator scattering at the endpoint of the twist-3 light-cone distribution amplitude (LCDA).

Phenomenologically, the QCD factorization (BBNS approach) has been applied to study many  $B$  meson decay modes, such as  $B \rightarrow D^{(*)}\pi^-$  [17,18],  $\pi\pi$ ,  $\pi K$  [19,20,14,16], and other interesting channels [21–24]. In particular, in a recent paper [16], Beneke *et al.* gave a detailed phenomenological analysis for  $B \rightarrow \pi\pi$  and  $\pi K$  within the frame of QCD factorization, in which the contributions from weak annihilation are also taken into account. In principle, weak annihilation is power suppressed within the frame of QCD factorization. Nevertheless, as emphasized in Ref. [25], these contributions may be numerically important for the decays  $B \rightarrow PP$ . An explicit calculation shows that there are very significant endpoint divergences in weak annihilation. This indicates that the weak annihilation may be dominated by the soft contributions. In Ref. [16], the authors give a phenomenological treatment of the endpoint divergences in both the hard spectator scattering and the weak annihilations. Such a treatment is really a *model-dependent* procedure. However, it may be helpful to estimate the importance of annihilation. The numerical results show that weak annihilation indeed gives evident corrections to the branching ratios of the decays  $B \rightarrow \pi\pi$  and  $\pi K$  in Ref. [16], and also causes very large uncertainties in the prediction. Assuming the universality of the endpoint divergence, the authors of Ref. [16] also gave a global fit for the CKM parameters by use of the branching

ratios of  $B \rightarrow \pi\pi$  and  $\pi K$  in the frame of QCD factorization, and derived a new constraint for the  $(\bar{\rho}, \bar{\eta})$  complex plane. The new constraint is slightly different from that derived by the other standard fit, but they are compatible with each other.

In this work, we will apply QCD factorization to all modes of  $B$  decay into two light pseudoscalar mesons, and give a careful and detailed analysis. For the decay modes  $B \rightarrow \pi\pi$  and  $\pi K$ , our work is actually a re-check of Beneke *et al.* [16], and we find that our results are consistent with theirs. The  $B \rightarrow P\eta^{(\prime)}$  has also been studied by M. Z. Yang and Y. D. Yang within the frame of QCD factorization [21]. The differences between their work and ours are that the other type twist-3 light-cone distribution amplitude  $\phi_\sigma$  is taken into account, which guarantees gauge invariance of our results; and the contributions from weak annihilation are also considered in our work. In addition, the digluon mechanism for the production of  $\eta^{(\prime)}$  is taken into account in Ref. [21]. Generally, it is believed that the anomalous coupling of  $\eta'g^*g^*$  can account for the large branching ratio of  $B \rightarrow K\eta'$ . However, whether the form factor  $\eta^{(\prime)}g^*g^*$  is perturbatively calculable or not is still an open question. In particular, at the endpoint of the light-cone distribution amplitudes (LCDAs), where the virtualities of the two gluons are both soft, the validity of the suppression from the LCDAs is questionable. Therefore, in our work, digluon mechanism is not considered although it can enhance the branching ratio of  $B \rightarrow K\eta'$ . For  $B \rightarrow KK$ , our work is totally new; the study of these decay modes is expected to give a constraint to the endpoint divergence in weak annihilation.

This paper is organized as follows. In Sect. II, we give a brief review of the effective Hamiltonian and QCD factorization including the chirally enhanced power corrections and weak annihilations. For a quantitative analysis of  $B \rightarrow PP$ , the necessary input parameters are discussed in Sect. III. In Sect. IV, the numerical results for the CP-averaged branching ratios and CP asymmetries for  $B \rightarrow PP$  are given and Sect. V is devoted to the conclusions.

## II. THEORETICAL FRAME FOR $B$ RARE DECAYS

### A. The effective Hamiltonian

$B$  decays involve three characteristic scales which are strongly ordered:  $m_W \gg m_b \gg \Lambda_{QCD}$ . How to separate or factorize these three scales is the most essential question in studying  $B$  hadronic decays.

With the operator product expansion method, the relevant  $|\Delta B| = 1$  effective Hamiltonian is given by [4]

$$\mathcal{H}_{eff} = \frac{G_F}{\sqrt{2}} \left[ \sum_{q=u,c} v_q \left( C_1(\mu) Q_1^q(\mu) + C_2(\mu) Q_2^q(\mu) + \sum_{k=3}^{10} C_k(\mu) Q_k(\mu) \right) - v_t \left( C_{7\gamma}(\mu) Q_{7\gamma}(\mu) + C_{8G}(\mu) Q_{8G}(\mu) \right) \right] + h.c., \quad (1)$$

where  $v_q = V_{qb}V_{qd}^*$  (for  $b \rightarrow d$  transition) or  $v_q = V_{qb}V_{qs}^*$  (for  $b \rightarrow s$  transition) and  $C_i(\mu)$  are the Wilson coefficients which have been evaluated to next-to-leading order with the perturbation theory and renormalization group method.

In the Eq.(1), the four-quark operators  $Q_i$  are given by

$$\begin{aligned}
Q_1^u &= (\bar{u}_\alpha b_\alpha)_{V-A} (\bar{q}_\beta u_\beta)_{V-A} & Q_1^c &= (\bar{c}_\alpha b_\alpha)_{V-A} (\bar{q}_\beta c_\beta)_{V-A} \\
Q_2^u &= (\bar{u}_\alpha b_\beta)_{V-A} (\bar{q}_\beta u_\alpha)_{V-A} & Q_2^c &= (\bar{c}_\alpha b_\beta)_{V-A} (\bar{q}_\beta c_\alpha)_{V-A} \\
Q_3 &= (\bar{q}_\alpha b_\alpha)_{V-A} \sum_{q'} (\bar{q}'_\beta q'_\beta)_{V-A} & Q_4 &= (\bar{q}_\beta b_\alpha)_{V-A} \sum_{q'} (\bar{q}'_\alpha q'_\beta)_{V-A} \\
Q_5 &= (\bar{q}_\alpha b_\alpha)_{V-A} \sum_{q'} (\bar{q}'_\beta q'_\beta)_{V+A} & Q_6 &= (\bar{q}_\beta b_\alpha)_{V-A} \sum_{q'} (\bar{q}'_\alpha q'_\beta)_{V+A} \\
Q_7 &= \frac{3}{2} (\bar{q}_\alpha b_\alpha)_{V-A} \sum_{q'} e_{q'} (\bar{q}'_\beta q'_\beta)_{V+A} & Q_8 &= \frac{3}{2} (\bar{q}_\beta b_\alpha)_{V-A} \sum_{q'} e_{q'} (\bar{q}'_\alpha q'_\beta)_{V+A} \\
Q_9 &= \frac{3}{2} (\bar{q}_\alpha b_\alpha)_{V-A} \sum_{q'} e_{q'} (\bar{q}'_\beta q'_\beta)_{V-A} & Q_{10} &= \frac{3}{2} (\bar{q}_\beta b_\alpha)_{V-A} \sum_{q'} e_{q'} (\bar{q}'_\alpha q'_\beta)_{V-A}
\end{aligned} \tag{2}$$

and

$$Q_{7\gamma} = \frac{e}{8\pi^2} m_b \bar{q}_\alpha \sigma^{\mu\nu} (1 + \gamma_5) b_\alpha F_{\mu\nu}, \quad Q_{8G} = \frac{g}{8\pi^2} m_b \bar{q}_\alpha \sigma^{\mu\nu} t_{\alpha\beta}^a (1 + \gamma_5) b_\beta G_{\mu\nu}^a, \quad (q = d \text{ or } s). \tag{3}$$

Here  $Q_1^q$  and  $Q_2^q$  are the tree operators,  $Q_3 - Q_6$  the QCD penguin operators,  $Q_7 - Q_{10}$  the electroweak penguin operators, and  $Q_{7\gamma}$  and  $Q_{8G}$  the magnetic-penguin operators.

In this effective Hamiltonian for  $B$  decays, the contributions from the large virtual momenta of the loop corrections from the scale  $\mu = \mathcal{O}(m_b)$  to  $m_W$  are given by the Wilson coefficients, and the low energy contributions are fully incorporated into the matrix elements of the operators [4]. So the derivation of the effective Hamiltonian can be called “the first step factorization”.

Several years ago, the perturbative corrections to the Wilson coefficients in the SM were evaluated to next-to-leading order with the renormalization group method. We list the numerical results in the naive dimensional regularization (NDR) scheme and at the three scales  $m_b/2$ ,  $m_b$  and  $2m_b$  in Table I.

## B. QCD factorization in the heavy quark limit

After “first step factorization”, the decay amplitude for  $B \rightarrow P_1 P_2$  can be written as

$$\mathcal{A}(B \rightarrow P_1 P_2) = \sum_i v_i C_i(\mu) \langle P_1 P_2 | Q_i(\mu) | B \rangle. \tag{4}$$

The central task now is to reliably evaluate the transition matrix element  $\langle P_1 P_2 | Q_i(\mu) | B \rangle$ . Note that the matrix element contains two scales:  $\mathcal{O}(m_b)$  and  $\Lambda_{QCD}$ . It is hoped that  $\langle P_1 P_2 | Q_i(\mu) | B \rangle$  can be separated into the short-distance contributions relating to large scale  $\mathcal{O}(m_b)$  and the long-distance contributions relating to the fundamental scale of QCD— $\Lambda_{QCD}$ . Then the short-distance contributions, which are perturbatively calculable, should recover the scheme and scale dependence of the hadronic matrix elements, and the long-distance contributions can be parameterized into some universal non-perturbative parameters.

In Ref. [13], Beneke, Buchalla, Neubert and Sachrajda show that this idea of factorization can be realized, at least at one-loop order, in the heavy quark limit. They argue that the emitted meson  $P_1$  carries large energy and momentum (about  $m_B/2$ ) and therefore can be described by leading-twist light-cone distribution amplitudes. It is natural to imagine that the soft gluons would decouple from the emitted  $P_1$  at leading order of

$\Lambda_{QCD}/m_b$  since the  $q\bar{q}$  pair in  $P_1$  form a small-size color dipole. However, the factorization requires that not only soft divergences, but also collinear divergences, should be cancelled. Fortunately, explicit calculations at one-loop order show that, in the heavy quark limit, all infrared divergences vanish after summing over the four vertex correction diagrams [Figs. 1(a)-1(d)]. As for the recoiled meson  $P_2$ , because the spectator quark in the  $B$  meson is transferred to it as a soft parton, Beneke *et al.* believe that, instead of light-cone distribution amplitudes, one should use nonperturbative form factors  $F^{BP_2}$  to describe it.<sup>1</sup> It should be noted that when the spectator quark interacts with one of the quarks in the emitted meson by a hard gluon exchange, the recoiling meson can be described by leading-twist distribution amplitudes. These hard spectator diagrams [Figs. 1(g),1(h)] can also be accounted for at the leading power of  $\Lambda_{QCD}/m_b$ . In summary, their factorization formula can be explicitly expressed as

$$\begin{aligned} \langle P_1 P_2 | Q_i | B \rangle &= F^{B \rightarrow P_2}(0) \int_0^1 dx T_i^I(x) \Phi_{P_1}(x) + \int_0^1 d\xi dx dy T_i^{II}(\xi, x, y) \Phi_B(\xi) \Phi_{P_1}(x) \Phi_{P_2}(y) \\ &= \langle P_1 P_2 | J_1 \otimes J_2 | B \rangle \cdot [1 + \sum r_n \alpha_s^n + \mathcal{O}(\Lambda_{QCD}/m_b)]. \end{aligned} \quad (5)$$

We call this factorization formalism as QCD factorization or the BBNS approach. In Eq.(5),  $\Phi_B(\xi)$  and  $\Phi_{P_i}(x)$  ( $i = 1, 2$ ) are the leading-twist wave functions of  $B$  and the light pseudoscalar mesons respectively, and  $T_i^{I,II}$  denote hard-scattering kernels which are calculable in perturbation theory. At the order of  $\alpha_s$ , the hard kernels  $T_i^{I,II}$  can be depicted by Fig. 1. Figures 1(a)-1(d) represent vertex corrections, Figs. 1(e) and 1(f) penguin corrections, and Figs. 1(g) and 1(h) hard spectator scattering.

Comparing this approach with naive factorization and/or generalized factorization, there are some interesting characteristics in the BBNS approach.

(i) At the leading order of  $\alpha_s$ , it can reproduce the results of naive factorization; at the higher order of  $\alpha_s$ , the renormalization scheme and scale dependence for the hadronic matrix elements can be recovered from the hard-scattering kernels  $T_i^I$ . The generalized factorization can also obtain the necessary dependence on scheme and scale. However, this dependence is based on one-loop calculations of quark-level matrix elements. According to Buras *et al.*, quark-level matrix elements are accompanied by infrared divergences. To avoid such divergences, one usually assumes that external quark states are off shell. Unfortunately, this will introduce gauge dependence, which is also unphysical. In Ref. [12], the authors give a calculation assuming the external quarks are on shell, and they show that the infrared singularities can be cancelled by assuming the final quarks are in the form of hadrons; their calculation is therefore gauge invariant. Their idea is almost the

---

<sup>1</sup>Light-cone sum rules also justify this nonperturbative property for the  $B$  to light form factors. It is different from the conclusion of Keum *et al.* [25]. In Ref. [25], the authors claim that the form factor  $F^{B\pi}(0)$  is perturbatively calculable in terms of the distribution amplitudes when the Sudakov  $k_T$  resummation and threshold resummation are taken into account. However, a recent detailed examination of such point of view by Descotes-Genon and Sachrajda shows that it is not justified [26]. They conclude that, the Sudakov form factors are not sufficient to suppress the contribution that comes from the nonperturbative region of large impact parameters, and therefore the form factor  $F^{B\pi}(0)$  is uncalculable in the standard hard-scattering approach.

same as the BBNS approach. The difference is that, in the BBNS approach, the ejected meson is represented as its light-cone distribution amplitude; in Ref. [12], the ejected  $q\bar{q}$  pair is in such a configuration that it is a color-singlet object and the quark shares almost the same momentum as the anti-quark. Because results in Ref. [12] are still from a calculation at the quark level, some information from the distributions of momentum fraction in hadrons is ignored.

(ii) Generalized factorization considers nonfactorizable contributions as intractable. Therefore, one may introduce one or more effective color numbers  $N_c^{eff}$  to phenomenologically represent nonfactorizable contributions. Furthermore,  $N_c^{eff}$  is assumed to be universal to maintain predictive power. However, QCD factorization tells us that the nonfactorizable contribution is indeed factorizable and therefore calculable in the heavy quark limit. In consequence,  $N_c^{eff}$  is calculable, and process dependent beyond the leading order of  $\alpha_s$ .

(iii) An interesting result of QCD factorization is that strong phases come solely from hard scattering processes and are therefore calculable in the heavy quark limit. From Eq.(5), it is easy to conclude that the imaginary part of decay amplitude arises only from hard scattering kernels  $T_i^f$  because nonperturbative form factors and light-cone distribution amplitudes are all real.  $T_i^f$  contains vertex corrections [Figs. 1 (a)-1(d)] and penguin corrections [Figs. 1(e),1(f)]. Strong phases from penguin corrections are commonly called the Bander-Silverman-Soni (BSS) mechanism [27], which is the unique source of strong phases in generalized factorization. However, the gluon virtuality of Fig. 1(e), which is well defined in QCD factorization, is ambiguous in generalized factorization and usually treated as a free parameter. In addition, vertex corrections will also contribute to strong phases in QCD factorization, which is missed in the generalized factorization.

(iv) Hard spectator contributions [Figs. 1(g),1(h)], which are leading power effects in QCD factorization, are missing in “naive factorization” and “generalized factorization”.

Readers are referred to Refs. [13,18] for more details.

### C. Chirally enhanced corrections in QCD factorization

It is observed that QCD factorization is demonstrated only in the strict heavy quark limit. This means that any generalization of QCD factorization to include or partly include power corrections of  $\Lambda_{QCD}/m_b$  should redemonstrate the factorization. There are a variety of sources which may contribute to power corrections in  $1/m_b$ ; examples are higher twist distribution amplitudes, transverse momenta of quarks in the light meson, annihilation diagrams, etc. Unfortunately, there is no known systematic way to evaluate these power corrections in general for exclusive decays. Moreover, factorization might break down when these power corrections, for instance transverse momenta effects, are considered. This indicates that one might have to give up the ambitious plan where all power corrections are, at least in principle, incorporated into QCD factorization order by order. One might argue that power corrections in  $B$  decays are numerically unimportant because these corrections are proportional to a small number  $\Lambda_{QCD}/m_b \simeq 1/15$ . But it is not true. For instance, the contributions of operator  $Q_6$  to decay amplitudes would formally vanish in the strict heavy quark limit. However it is numerically very important in penguin-dominant  $B$  rare decays, such as the interesting channels  $B \rightarrow \pi K$ , etc. This is because  $Q_6$  is always multiplied by a formally power suppressed but chirally enhanced

factor  $r_\chi = 2m_P^2/(m_b(m_1 + m_2)) \sim \mathcal{O}(1)$ , where  $m_1$  and  $m_2$  are current quark masses. So power suppression might probably fail at least in this case. Therefore phenomenological applicability of QCD factorization in B rare decays requires at least a consistent inclusion of chirally enhanced corrections.

The chirally enhanced corrections arise from twist-3 light-cone distribution amplitudes, generally called  $\phi_p(x)$  and  $\phi_\sigma(x)$ . For light pseudoscalar mesons, they are defined as [28]

$$\langle P(p') | \bar{q}(y) i\gamma_5 q(x) | 0 \rangle = f_P \mu_P \int_0^1 du e^{i(u p' \cdot y + \bar{u} p' \cdot x)} \phi_p(u), \quad (6)$$

$$\langle P(p') | \bar{q}(y) \sigma_{\mu\nu} \gamma_5 q(x) | 0 \rangle = i f_P \mu_P (p'_\mu z_\nu - p'_\nu z_\mu) \int_0^1 du e^{i(u p' \cdot y + \bar{u} p' \cdot x)} \frac{\phi_\sigma(u)}{6}, \quad (7)$$

where  $\mu_p = \frac{m_p^2}{m_1 + m_2}$ ,  $z = y - x$ , and  $m_1$  and  $m_2$  are the corresponding current quark masses. So, when chirally enhanced corrections are concerned, the final light mesons should be described by leading twist and twist-3 distribution amplitudes [29]:

$$\begin{aligned} \langle P(p') | \bar{q}_\alpha(y) q_\delta(x) | 0 \rangle &= \frac{i f_P}{4} \int_0^1 du e^{i(u p' \cdot y + \bar{u} p' \cdot x)} \\ &\times \left\{ \not{p}' \gamma_5 \phi(u) - \mu_P \gamma_5 \left( \phi_p(u) - \sigma_{\mu\nu} p'^\mu z^\nu \frac{\phi_\sigma(u)}{6} \right) \right\}_{\delta\alpha}. \end{aligned} \quad (8)$$

Thus it is crucial to show that factorization really holds when considering twist-3 distribution amplitudes. The most difficult part is to demonstrate the infrared finiteness of the hard scattering kernels  $T_i^J$ . For more technical details of this proof, readers are referred to the literature [15,16].

With the effective Hamiltonian and QCD factorization formula,  $B \rightarrow P_1 P_2$  decay amplitudes in QCD factorization can be written as

$$A(B \rightarrow P_1 P_2) = \frac{G_F}{\sqrt{2}} \sum_{p=u,c} \sum_{i=1,10} v_p a_i^p \langle P_1 P_2 | Q_i | B \rangle_F, \quad (9)$$

where  $v_p$  is the CKM factor,  $\langle P_1 P_2 | Q_i | B \rangle_F$  is the factorized matrix element and is the same as the definition of the BSW Lagrangian [5]. The explicit expressions for the decay amplitudes of  $B \rightarrow P_1 P_2$  are listed in the Appendixes of [11,12].

For illustration, we give the explicit expressions of  $a_i^p$  ( $i = 1$  to 10) for  $B \rightarrow \pi\pi$  (using symmetric LCDAs of the pion). It is easy to generalize these formulas to the case that the final states are other light pseudoscalars. Furthermore, we take only some of QED corrections into account in our final formula, in particular the QED penguin insertions. Now  $a_i^p$  for  $B \rightarrow \pi\pi$  in NDR  $\gamma_5$  scheme is listed as follows:

$$a_1^u = C_1 + \frac{C_2}{N} + \frac{\alpha_s}{4\pi} \frac{C_F}{N} C_2 F, \quad (10)$$

$$a_2^u = C_2 + \frac{C_1}{N} + \frac{\alpha_s}{4\pi} \frac{C_F}{N} C_1 F, \quad (11)$$

$$a_3 = C_3 + \frac{C_4}{N} + \frac{\alpha_s}{4\pi} \frac{C_F}{N} C_4 F, \quad (12)$$

$$\begin{aligned} a_4^p &= C_4 + \frac{C_3}{N} + \frac{\alpha_s}{4\pi} \frac{C_F}{N} C_3 F \\ &- \frac{\alpha_s}{4\pi} \frac{C_F}{N} \left\{ C_1 \left( \frac{4}{3} \log \frac{\mu}{m_b} + G(s_p) - \frac{2}{3} \right) + \left( C_3 - \frac{C_9}{2} \right) \left( \frac{8}{3} \log \frac{\mu}{m_b} + G(0) + G(1) - \frac{4}{3} \right) \right\} \end{aligned}$$



$$+ \sum_{q=u,d,s,c,b} (C_4 + C_6 + \frac{3}{2}e_q C_8 + \frac{3}{2}e_q C_{10}) \left( \frac{4}{3} \log \frac{\mu}{m_b} + G(s_q) \right) + G_8 C_{8G} \Big\}, \quad (13)$$

$$a_5 = C_5 + \frac{C_6}{N} + \frac{\alpha_s}{4\pi} \frac{C_F}{N} C_6 (-F - 12), \quad (14)$$

$$\begin{aligned} a_6^p &= C_6 + \frac{C_5}{N} - \frac{\alpha_s}{4\pi} \frac{C_F}{N} 6C_5 \\ &\quad - \frac{\alpha_s}{4\pi} \frac{C_F}{N} \left\{ C_1 \left( \left(1 + \frac{2}{3}A_\sigma\right) \log \frac{\mu}{m_b} - \frac{1}{2} - \frac{1}{3}A_\sigma + G'(s_p) + G^\sigma(s_p) \right) \right. \\ &\quad + \sum_{q=d,b} (C_3 - \frac{C_9}{2}) \left( \left(1 + \frac{2}{3}A_\sigma\right) \log \frac{\mu}{m_b} - \frac{1}{2} - \frac{1}{3}A_\sigma + G'(s_q) + G^\sigma(s_q) \right) \\ &\quad + \sum_{q=u,d,s,c,b} (C_4 + C_6 + \frac{3}{2}e_q C_8 + \frac{3}{2}e_q C_{10}) \left( \left(1 + \frac{2}{3}A_\sigma\right) \log \frac{\mu}{m_b} + G'(s_q) + G^\sigma(s_q) \right) \\ &\quad \left. + \left( \frac{3}{2} + A_\sigma \right) C_{8G} \right\}, \quad (15) \end{aligned}$$

$$a_7 = C_7 + \frac{C_8}{N} + \frac{\alpha_s}{4\pi} \frac{C_F}{N} C_8 (-F - 12), \quad (16)$$

$$\begin{aligned} a_8^p &= C_8 + \frac{C_7}{N} - \frac{\alpha_s}{4\pi} \frac{C_F}{N} 6C_7 \\ &\quad - \frac{\alpha_{em}}{9\pi} \left\{ (C_2 + \frac{C_1}{N}) \left( \left(1 + \frac{2}{3}A_\sigma\right) \log \frac{\mu}{m_b} - \frac{1}{2} - \frac{1}{3}A_\sigma + G'(s_p) + G^\sigma(s_p) \right) \right. \\ &\quad + (C_4 + \frac{C_3}{N}) \sum_{q=d,b} \frac{3}{2}e_q \left( \left(1 + \frac{2}{3}A_\sigma\right) \log \frac{\mu}{m_b} - \frac{1}{2} - \frac{1}{3}A_\sigma + G'(s_q) + G^\sigma(s_q) \right) \\ &\quad + (C_3 + \frac{C_4}{N} + C_5 + \frac{C_6}{N}) \sum_{q=u,d,s,c,b} \frac{3}{2}e_q \left( \left(1 + \frac{2}{3}A_\sigma\right) \log \frac{\mu}{m_b} + G'(s_q) + G^\sigma(s_q) \right) \\ &\quad \left. + \left( \frac{3}{4} + \frac{1}{2}A_\sigma \right) C_{7\gamma} \right\}, \quad (17) \end{aligned}$$

$$a_9 = C_9 + \frac{C_{10}}{N} + \frac{\alpha_s}{4\pi} \frac{C_F}{N} C_{10} F, \quad (18)$$

$$\begin{aligned} a_{10}^p &= C_{10} + \frac{C_9}{N} + \frac{\alpha_s}{4\pi} \frac{C_F}{N} C_9 F - \frac{\alpha_{em}}{9\pi} \left\{ (C_2 + \frac{C_1}{N}) \left( \frac{4}{3} \log \frac{\mu}{m_b} + G(s_p) - \frac{2}{3} \right) \right. \\ &\quad + (C_4 + \frac{C_3}{N}) \sum_{q=d,b} \frac{3}{2}e_q \left( \frac{4}{3} \log \frac{\mu}{m_b} + G(s_q) - \frac{2}{3} \right) \\ &\quad \left. + (C_3 + \frac{C_4}{N} + C_5 + \frac{C_6}{N}) \sum_{q=u,d,s,c,b} \frac{3}{2}e_q \left( \frac{4}{3} \log \frac{\mu}{m_b} + G(s_q) \right) + \frac{1}{2} G_8 C_{7\gamma} \right\}. \quad (19) \end{aligned}$$

Here  $N = 3$  is the color number,  $C_F = (N^2 - 1)/2N$  is the color factor,  $s_q = m_q^2/m_b^2$ , and we define the other symbols in the above expressions as

$$F = -12 \ln \frac{\mu}{m_b} - 18 + f^I + f^{II}, \quad (20)$$

$$f^I = \int_0^1 dx g(x) \phi(x), \quad G_8 = \int_0^1 dx G_8(x) \phi(x), \quad (21)$$

$$G(s) = \int_0^1 dx G(s, x) \phi(x), \quad (22)$$

$$G'(s) = \int_0^1 dx G'(s, x) \phi_p(x), \quad (23)$$

$$G^\sigma(s) = \int_0^1 dx G^\sigma(s, x) \frac{\phi_\sigma(x)}{6(1-x)}, \quad A_\sigma = \int_0^1 dx \frac{\phi_\sigma(x)}{6(1-x)}, \quad (24)$$

where  $\phi(x)$  [ $\phi_p(x)$ ,  $\phi_\sigma(x)$ ] is leading twist (twist-3) LCDA of the ejected pion, and the hard-scattering functions are

$$g(x) = 3 \frac{1-2x}{1-x} \ln x - 3i\pi, \quad G_8(x) = \frac{2}{1-x}, \quad (25)$$

$$G(s, x) = -4 \int_0^1 du u(1-u) \ln(s - u(1-u)(1-x) - i\epsilon), \quad (26)$$

$$G'(s, x) = -3 \int_0^1 du u(1-u) \ln(s - u(1-u)(1-x) - i\epsilon), \quad (27)$$

$$G^\sigma(s, x) = -2 \int_0^1 du u(1-u) \ln(s - u(1-u)(1-x) - i\epsilon) \\ + \int_0^1 du \frac{u^2(1-u)^2(1-x)}{s - u(1-u)(1-x) - i\epsilon}. \quad (28)$$

The contributions from the hard spectator scattering [Figs. 1(g), 1(h)] are reduced to the factor  $f^{II}$ :

$$f^{II} = \frac{4\pi^2}{N} \frac{f_\pi f_B}{F_+^{B \rightarrow \pi}(0) m_B^2} \int_0^1 d\xi \frac{\Phi_B(\xi)}{\xi} \int_0^1 dx \frac{\phi(x)}{x} \int_0^1 dy \left[ \frac{\phi(y)}{1-y} + \frac{2\mu_\pi}{M_B} \frac{\phi_\sigma(y)}{6(1-y)^2} \right]. \quad (29)$$

There is a divergent integral in  $f^{II}$ . When we do numerical calculation in this work, we will simply parameterize this divergence as what was done by Beneke *et al.* [14]:

$$X_H = \int dy/y = \ln(m_b/\Lambda_{QCD}) + \varrho_H e^{i\phi_H}, \quad (30)$$

where  $\phi_H$  is an arbitrary phase,  $0^\circ \leq \phi_H \leq 360^\circ$ , and  $\varrho_H$  is varied from 0 to 3 (realistic) or 6 (conservative).<sup>2</sup>

---

<sup>2</sup>This parameterization is a little bit different from that in the recent paper [16] by Beneke *et al.*, but the variation of these two parameterization are almost the same. In addition, we pointed out in [15] that  $f^{II}$  might be convergent if the transverse momentum  $k_T$  of the parton is taken into account and the Sudakov resummation is invoked. In Ref. [30], the authors find that value of  $f^{II}$  is really in the range of the above parameterization when the Sudakov suppression is taken into account. In recent literature [31] of the perturbative QCD (PQCD) method, the authors point out that the threshold resummation can also help to suppress the endpoint singularities, especially for the twist-3 level. However, this treatment contradicts the claim of Descotes-Genon

We illustrate numerically the scale dependence of  $a_i^p$  in Table II. Here we use the asymptotic form of the LCDAs of the light pseudoscalar meson, which are

$$\phi(x) = 6x(1-x), \quad (31)$$

$$\phi_p(x) = 1, \quad (32)$$

$$\phi_\sigma(x) = 6x(1-x), \quad (33)$$

and we set  $f^{II} = 0$  in computation because of its uncertainty.

From the expressions and numerical results of the coefficients  $a_i$ , some general observations are listed below.

(1)  $a_i$  ( $i = 1 - 5, 7, 9, 10$ ) and  $a_{6,8}r_\chi$  are RG invariant so they guarantee a full decay amplitude independent of the renormalization scale. We have shown that the coefficients  $a_i$  ( $i = 1 - 5, 7, 9, 10$ ) are renormalization scale independent at the order of  $\alpha_s$  with asymptotic LCDAs in [15],

$$\frac{da_i}{d\ln\mu} = 0 \quad (i \neq 6, 8),$$

However,  $a_6$  and  $a_8$  must be scale dependent because the factorized matrix elements multiplied by  $a_6$  and  $a_8$  are scale-dependent. But,

$$\frac{d(a_i r_\chi)}{d\ln\mu} = 0 \quad (i = 6, 8).$$

This point can also be seen roughly from numerical results in Table II. It should be noted that the imaginary part of  $a_i$  is at the order of  $\alpha_s$ , and its remaining scale dependence must be cancelled by the radiative corrections from higher order of  $\alpha_s$ .

(2) The coefficients  $a_i$  are gauge invariant. At the leading power of  $\Lambda_{QCD}/m_b$ , the light meson is represented as its leading twist light-cone wave function (LCWF). In the calculation, the Dirac structure of the leading twist LCWF guarantees that the light meson can be taken as a pair of collinear on-shell massless quark and antiquark. Therefore, the on-shell condition guarantees the gauge invariance of  $a_i$  ( $i \neq 6, 8$ ). In Ref. [16], the authors have shown that at the twist-3 level the light meson can be also taken as a pair of on-shell massless quark and anti-quark when the asymptotic form of twist-3 LCDAs are taken. Then,  $a_{6,8}$  are also independent of the gauge choice.

(3) The quantities of  $a_1, a_2$  receive a special attention, because they are related to tree operators  $Q_{1,2}$ , so they are numerically large. QCD penguins effects are incorporated to the coefficients  $a_{3-6}$ , in which  $a_{3,5}$  are smaller than  $a_{4,6}$ , and  $a_3 + a_5$  is  $\mathcal{O}(10^{-4})$ .  $a_{4,6}$  have the same order as  $a_2$ , so they will play a dominant role when the effects of tree operators are CKM-suppressed, for example in the  $b \rightarrow s$  transition. The electroweak penguin coefficients  $a_7 - a_{10}$  are even smaller.  $a_9$  is the largest one among them, and numerically comparable with the QCD penguin coefficients  $a_{3,5}$ . Thus,  $a_9$  may play an important role in some decay modes, such as  $B \rightarrow \pi^0 K$ .

---

and Sachrajda. They conclude in Ref. [26] that it is impossible to make reliable predictions for power corrections to the amplitudes for exclusive two-body  $B$  decays which have end-point singularities, even if the Sudakove effects are taken into account. We think that this point of view needs further careful investigation.

(4) The imaginary part of  $a_i$  arises from the radiative corrections. Unlike in the generalized factorization, the imaginary part of  $a_i$  comes not only from the penguin corrections (BSS mechanism), but also from the vertex corrections. However, it is suppressed by  $\alpha_s$ , and generally numerically small. Thus, the strong phases evaluated from the BBNS approach are generally small. But in some special cases the situation will be different. For example, the imaginary parts of  $a_{2,4,6}$ , especially for  $a_2$ , are larger than those of the other coefficients, so, when their contributions are dominant in some decay modes, strong interaction phases might be large, which would result in a large CP violation.

#### D. Contributions of annihilation amplitudes

Annihilation contributions appear in almost all charmless decay modes  $B \rightarrow PP$ . In some cases, they may be important in spite of the power suppression. As emphasized in the PQCD method [25,32], weak annihilation can give a large imaginary part to the decay amplitudes. Then, within the framework of the PQCD method, large CP violations are expected. In this work, we will follow Beneke *et al.* [16], writing the annihilation contributions in terms of convolutions of “hard-scattering” kernels with LCDAs by ignoring the soft endpoint divergences. This kind of treatment is obviously not self-consistent; however, it can help us to give an estimation of the annihilation. The corresponding diagrams of weak annihilation are depicted in Fig. 2. Here, we will follow the convention in Ref. [16]:

$$\mathcal{A}^{ann}(B \rightarrow P_1 P_2) \propto f_B f_{P_1} f_{P_2} \sum v_i r b_i \quad (34)$$

The decay amplitudes of weak annihilation for  $B \rightarrow PP$  are listed in the Appendix.

Similar to the treatment for the endpoint divergence in hard spectator scattering, we also parameterize the endpoint divergence  $X_A$  in the weak annihilation as follows:

$$X_A = \int dy/y = \ln(m_b/\Lambda_{QCD}) + \varrho_A e^{i\phi_A}, \quad (35)$$

where  $\phi_A$  is an arbitrary phase,  $0^\circ \leq \phi_A \leq 360^\circ$ , and  $\varrho_A$  is varied from 0 to 3 (realistic) or 6 (conservative). It should be noted that there is no correlation between  $X_A$  and  $X_H$  for their different origins.

We will apply the above formulae to revisit rare  $B$  decays in what follows.

### III. INPUT PARAMETERS

The decay amplitude for  $B \rightarrow PP$  can be expressed by various parameters, such as the CKM matrix elements, form factors, Wilson coefficients  $C_i(\mu)$ , LCDAs, and so on. The values of these parameters will affect our predictions for CP-averaged branching ratios and CP-violating asymmetries. Now we will specify them for use in calculation.

#### A. CKM matrix elements

The CKM matrix in the Wolfenstein parameterization reads

$$V_{CKM} = \begin{pmatrix} 1 - \lambda^2/2 & \lambda & A\lambda^3(\rho - i\eta) \\ -\lambda & 1 - \lambda^2/2 & A\lambda^2 \\ A\lambda^3(1 - \rho - i\eta) & -A\lambda^2 & 1 \end{pmatrix} + \mathcal{O}(\lambda^4). \quad (36)$$

Here we take the Wolfenstein parameters from the fit of Ciuchini et al. [33]:  $A = 0.819 \pm 0.040$ ,  $\lambda = 0.2237 \pm 0.0033$ ,  $\bar{\rho} = \rho(1 - \lambda^2/2) = 0.224 \pm 0.038$ ,  $\bar{\eta} = \eta(1 - \lambda^2/2) = 0.317 \pm 0.040$  and  $\gamma = (54.8 \pm 6.2)^\circ$ . Correspondingly, we have  $\rho = 0.230 \pm 0.039$ ,  $\eta = 0.325 \pm 0.039$ , and  $\sqrt{\rho^2 + \eta^2} = 0.398 \pm 0.040$ . If not stated otherwise, we shall use the central values as the default values.

## B. Form factors and decay constants

Decay constants and heavy-to-light form factors are defined by following current matrix elements:

$$\langle P(q) | \bar{q}_1 \gamma_\mu \gamma_5 q_2 | 0 \rangle = -i f_P q_\mu, \quad (37)$$

$$\begin{aligned} \langle P(q) | \bar{q} \gamma_\mu b | B \rangle &= \left[ (p+q)_\mu - \frac{m_B^2 - m_P^2}{(p-q)^2} (p-q)_\mu \right] F_1((p-q)^2) \\ &+ \frac{m_B^2 - m_P^2}{(p-q)^2} (p-q)_\mu F_0((p-q)^2). \end{aligned} \quad (38)$$

For the decay constants we use  $f_\pi = 131$  MeV,  $f_K = 160$  MeV, and  $f_B = 180 \pm 40$  MeV. As to the decay constants related to the  $\eta$  and  $\eta'$ , we shall take the convention in [11,12]:

$$\langle 0 | \bar{q} \gamma^\mu \gamma_5 q | \eta^{(\prime)}(p) \rangle = i f_{\eta^{(\prime)}}^q p^\mu,$$

and

$$\langle 0 | \bar{s} \gamma_5 s | \eta^{(\prime)}(p) \rangle = -i \frac{(f_{\eta^{(\prime)}}^s - f_{\eta^{(\prime)}}^u) m_{\eta^{(\prime)}}^2}{2m_s},$$

$$\langle 0 | \bar{u} \gamma_5 u | \eta^{(\prime)}(p) \rangle = \langle 0 | \bar{d} \gamma_5 d | \eta^{(\prime)}(p) \rangle = \frac{f_{\eta^{(\prime)}}^u}{f_{\eta^{(\prime)}}^s} \langle 0 | \bar{s} \gamma_5 s | \eta^{(\prime)}(p) \rangle.$$

Here we shall not consider the charm quark content in  $\eta^{(\prime)}$ . The relations between  $\eta$ - $\eta'$  mixing and  $\eta_8$ - $\eta_0$  [the  $SU(3)$  octet and singlet] are

$$|\eta\rangle = \cos \theta_8 |\eta_8\rangle - \sin \theta_0 |\eta_0\rangle, \quad |\eta'\rangle = \sin \theta_8 |\eta_8\rangle + \cos \theta_0 |\eta_0\rangle, \quad (39)$$

$$f_\eta^u = \frac{f_8}{\sqrt{6}} \cos \theta_8 - \frac{f_0}{\sqrt{3}} \sin \theta_0, \quad f_{\eta'}^u = \frac{f_8}{\sqrt{6}} \sin \theta_8 + \frac{f_0}{\sqrt{3}} \cos \theta_0, \quad (40)$$

$$f_\eta^s = -2 \frac{f_8}{\sqrt{6}} \cos \theta_8 - \frac{f_0}{\sqrt{3}} \sin \theta_0, \quad f_{\eta'}^s = -2 \frac{f_8}{\sqrt{6}} \sin \theta_8 + \frac{f_0}{\sqrt{3}} \cos \theta_0, \quad (41)$$

Here  $f_8, f_0$  are decay constants of  $\eta_8, \eta_0$  respectively,  $\theta_8, \theta_0$  are the mixing angles. Their values are [34]  $f_8 \approx 1.28f_\pi \approx 168$  MeV,  $f_0 \approx 1.20f_\pi \approx 157$  MeV,  $\theta_8 \approx -22.2^\circ$ , and  $\theta_0 \approx -9.1^\circ$ .

We take  $F_0^{B\pi} = 0.28 \pm 0.05$ , which is obtained by the light-cone sum rule [10]. For  $B \rightarrow K, \eta^{(\prime)}$  transitions, the following relations are applied to give their corresponding values:

$$\frac{f_\pi}{f_K} \approx \frac{F_0^{B\pi}(0)}{F_0^{BK}(0)}, \quad F_{0,1}^{B\eta} = F_{0,1}^{B\pi} \left( \frac{\cos\theta_8}{\sqrt{6}} - \frac{\sin\theta_0}{\sqrt{3}} \right), \quad F_{0,1}^{B\eta'} = F_{0,1}^{B\pi} \left( \frac{\sin\theta_8}{\sqrt{6}} + \frac{\cos\theta_0}{\sqrt{3}} \right). \quad (42)$$

### C. Quark masses

There are two types of quark mass in our analysis. One type is the pole mass which appears in the loop integration. Accompanied by the  $\mathcal{O}(\alpha_f)$  corrections to the hadronic matrix elements, the pole masses contribute to coefficients  $a_i$  through the functions  $G(s, x)$ ,  $G'(s, x)$  and  $G^\sigma(s, x)$ , or  $G(s)$ ,  $G'(s)$  and  $G^\sigma(s)$ . Here we fix them as

$$m_u = m_d = m_s = 0, \quad m_c = 1.45\text{GeV}, \quad m_b = 4.6\text{GeV}.$$

The other type quark mass appears in the hadronic matrix elements and the chirally enhanced factor  $r_\chi$  through the equations of motion. They are renormalization scale dependent. And their values have been summarized in [35]. Here we shall use the 2000 Particle Data Group (PDG2000) data for discussion:

$$\bar{m}_b(\bar{m}_b) = 4.0 \sim 4.4\text{GeV}, \quad \bar{m}_s(2\text{GeV}) = 75 \sim 170\text{MeV},$$

$$\bar{m}_d(2\text{GeV}) = 3 \sim 9\text{MeV}, \quad \bar{m}_u(2\text{GeV}) = 1 \sim 5\text{MeV}.$$

Here, we take the central values of the  $b$  quark and  $s$  quark as default values. Because the current masses of light quarks are difficult to fix, we would like to take

$$r_{\eta^{(\prime)}} \left( 1 - \frac{f_{\eta^{(\prime)}}^u}{f_{\eta^{(\prime)}}^s} \right) = r_\pi = r_K = r_\chi.$$

We think that it is a good approximation in our calculation. Using the renormalization group equation, we can get the corresponding running  $r_\chi$  at the scale  $\mu = \mathcal{O}(m_b)$ :

$$r_\chi(m_b/2) = 0.85, \quad r_\chi(m_b) = 1.14, \quad r_\chi(2m_b) = 1.42.$$

## IV. NUMERICAL ANALYSIS

### A. Branching ratios and comparison with data

In the  $B$  meson rest frame, we have two-body decay width

$$\Gamma(B \rightarrow P_1 P_2) = \frac{1}{8\pi} \frac{|p|}{m_B^2} |\mathcal{A}(B \rightarrow P_1 P_2)|^2, \quad (43)$$

where

$$|p| = \frac{\sqrt{[m_B^2 - (m_{P_1} + m_{P_2})^2][m_B^2 - (m_{P_1} - m_{P_2})^2]}}{2m_B}.$$

The corresponding branching ratio is

$$\text{BR}(B \rightarrow P_1 P_2) = \frac{\Gamma(B \rightarrow P_1 P_2)}{\Gamma_{tot}}, \quad (44)$$

where  $\tau = 1/\Gamma_{tot}$ . In our calculation, we take  $\tau = 1.548 \times 10^{-12}$  sec for  $B^0$ , and  $\tau = 1.653 \times 10^{-12}$  sec for  $B^\pm$ . In addition, because we work in the heavy quark limit, we take the mass of light meson as zero in the computation of phase space; then  $|p| = m_B/2$ .

We show experimental data and theoretical predictions for the CP-averaged branching ratios for  $B \rightarrow PP$  in Table III and Table IV, respectively. In Table IV, we give the averages of the branching ratios of  $B \rightarrow PP$  and their CP-conjugate modes with the default values of the parameters at three different renormalization scales  $\mu = m_b/2, m_b, 2m_b$ . From Table III and Table IV some remarks are in order.

(1) For the decay modes  $B \rightarrow \pi\pi$  and  $B \rightarrow \pi K$ , our predictions are consistent with those by Beneke *et al.* [16]. In these modes, with the default values of the parameters, we find that the CP-averaged branching ratios of  $B^\pm \rightarrow \pi^0\pi^-$  ( $\simeq$  pure tree) and  $B^\pm \rightarrow K^0\pi^\pm$  (pure penguin) are in good agreement with the experimental measurements. Therefore these two decay modes can be considered as good probes of QCD factorization for  $B$  meson decays to two light mesons [36]. For the other modes  $B \rightarrow \pi\pi$  and  $B \rightarrow \pi K$ , the predictions of the CP-averaged branching ratios obtained by using the default values of the parameters seem not very good compared with the experimental measurements. In particular, the theoretical prediction for the branching ratio of  $B^0 \rightarrow \pi^+\pi^-$  is larger than the experimental data. The same situation also occurs in generalized factorization [11,12]. For the other decays modes  $B \rightarrow \pi K$ , our predictions seem smaller than the measurements. But taking the uncertainties of the input parameters into account, such as the CKM matrix elements (especially the angle  $\gamma$  and  $|V_{ub}|$ ), the endpoint divergences in hard spectator scattering and weak annihilations, form factors, etc., it is possible that the theoretical predictions from the BBNS approach can be in accord with the experimental results. In Refs. [37,36], the author gave a global fit to the CP-averaged branching ratios of  $B \rightarrow \pi\pi, \pi K$  within the framework of the QCD factorization. With the best fit values, the branching ratios of  $B \rightarrow \pi\pi$  and  $\pi K$  are in very good agreement with the experimental measurements very well. [Although, in the best fit, value of  $\gamma$  is slightly too large (about  $90^\circ$ ) and  $|V_{ub}|$  is comparably small, they are still compatible with the standard fit using semileptonic decays,  $K - \bar{K}$  mixing and  $B - \bar{B}$  mixing.]

(2) We note that experimental data for CP-averaged branching ratios for  $B \rightarrow K\eta'$  are about four times larger than our theoretical predictions with default values of the parameters. The results under the generalized factorization (GF) framework are similar [11,12]. In Refs. [11,12], the charm quark content in  $\eta'$  is considered; however, this mechanism cannot give a good explanation for experimental data yet. The unexpectedly large data have triggered considerable theoretical interest in understanding the mechanism of  $\eta'$  production, and have been widely discussed in the literature [38]. So far, it is generally assumed that digluon fusion mechanism could enhance  $\eta'$  production, but the shape of form factor of the vertex  $g^*g^*\eta'$  brings a very large uncertainty to predictions of the

contribution from digluon mechanism [39]. Recently, M.Z. Yang and Y.D. Yang gave a calculation for  $B \rightarrow \eta^{(\prime)}P$  within the framework of the BBNS approach [21], in which the digluon mechanism is considered. In that paper, the authors compute the vertex of  $g^*g^*\eta'$  in perturbative QCD, and find the branching ratios of  $B \rightarrow K\eta'$  are really enhanced and in agreement with the experimental measurement. But, as mentioned in our Introduction, we think that the consistency of their perturbative calculation is questionable due to the endpoint behavior.

(3) For the decays  $B^\pm \rightarrow \pi^\pm\eta^{(\prime)}$ ,  $K^\pm\eta$ , the CP-averaged branching ratios predicted by the BBNS approach are at the order of  $10^{-6}$ . We expect that these decay modes can be observed soon at the BaBar and Belle experiments <sup>3</sup>.

(4) For the decays  $B^0 \rightarrow \pi^0\pi^0$ ,  $\pi^0\eta^{(\prime)}$ ,  $\eta^{(\prime)}\eta^{(\prime)}$ , our predictions show that their CP-averaged branching ratios are very small and about  $\mathcal{O}(10^{-7}) \sim \mathcal{O}(10^{-8})$ . If these predictions are reliable, it is very hard to observe these decay modes at the BaBar and Belle experiments.

(5) In the BBNS approach, the predictions for the branching ratios of  $B \rightarrow KK$  are highly suppressed, especially for  $B^0 \rightarrow K^+K^-$ , which is purely from the weak annihilation contributions. In Ref. [40], the authors evaluate the decays  $B \rightarrow KK$  by use of the PQCD method, and also found that their branching ratios are very small. These decay modes can be a good probe for long-distance final state interaction (FSI). On the other hand, as we show in the Appendix, if the endpoint divergence  $X_A$  is universal, the measurement for the branching ratio of  $B^0 \rightarrow K^+K^-$  may give a constraint for the range of  $X_A$ .

In Table IV, for comparison, we also give the estimations for the CP-averaged branching ratios of  $B \rightarrow PP$  using the naive factorization (NF) approximation. Again, we list the predictions by the BBNS approach with and without considering the weak annihilation also. From these results, some general observations are given as follows.

Obviously, predictions on branching ratios for  $B \rightarrow PP$  using the BBNS approach are less scale dependent compared with those in the NF framework, especially in the  $b \rightarrow s$  transition, such as  $B \rightarrow K\pi$ ,  $K\eta^{(\prime)}$ . Noting that  $a_i$  are calculated at one-loop level, if the corrections from high order of  $\alpha_s$  were taken into account, the scale dependence of theoretical predictions might be further reduced.

Generally, the contributions from weak annihilation are highly power suppressed. However, due to the endpoint divergences, they may give observable contributions in our results. In  $B \rightarrow \pi K$ , we can see that the weak annihilation can give about 5%  $\sim$  10% enhancement. Note that the results of Table IV are computed by the default parameters. If we varied the parameters for the endpoint divergences in weak annihilations, it would give much larger uncertainties to our predictions. This will be shown in the next subsection in detail.

---

<sup>3</sup>Recently, Belle and BaBar collaborations report their measurements of the branching ratio of the decay  $B^\pm \rightarrow \pi^\pm\eta'$  which is consistent with zero. The 90% CL upper limit is  $\text{BR}(B^\pm \rightarrow \pi^\pm\eta') < 7 \times 10^{-6}$  (at Belle) or  $\text{BR}(B^\pm \rightarrow \pi^\pm\eta') < 12 \times 10^{-6}$  (at BaBar).



## B. Uncertainty of predictions

In Fig. 3, based on the BBNS approach, we show the dependence of branching ratios for  $B \rightarrow \pi\pi$ ,  $\pi K$  and  $K\eta'$  on the weak phase  $\gamma$ , scanning all ranges of the variation of parameters, including the CKM matrix elements, form factors, endpoint divergence  $\int_0^1 dx/x$ , and so on. Note that weak annihilation effects do not contribute to  $B^\pm \rightarrow \pi^\pm\pi^0$ . We can see that our theoretical predictions give very wide dot shades for the branching ratios within the range of parameters. So it is possible that the predictions for CP-averaged branching ratios of the decays  $B \rightarrow \pi\pi$ ,  $\pi K$  are simultaneously consistent with the experimental data by use of the same input parameters. The results of the global fit in Refs. [16,36,37] show that, with the best fit values of the input parameters and within the framework of QCD factorization, the predictions for the branching ratios of  $B \rightarrow \pi\pi$  and  $\pi K$  can fit the experimental data simultaneously with good  $\chi^2/n_{dof}$ .

In Fig. 4, we show the dependence of the CP-averaged branching ratios of  $B^0 \rightarrow \pi^0 K^0$ ,  $B^\pm \rightarrow K^\pm\pi^0$  and  $B^0 \rightarrow \pi^+\pi^-$  on the CKM matrix elements, form factors, and endpoint divergence in hard spectator scattering and weak annihilations. From Fig. 4, some remarks are given in order.

For the decays  $B^0 \rightarrow \pi^0 K^0$  and  $B^\pm \rightarrow K^\pm\pi^0$ , the CP-averaged branching ratios weakly depend on  $|V_{ub}/V_{cb}|$  because that the decays  $B \rightarrow \pi K$  are dominated by penguin diagrams and  $|v_u/v_c| = |(V_{us}^*V_{ub})/(V_{cs}^*V_{cb})|$  is highly suppressed by  $\mathcal{O}(\lambda^2)$  in the  $b \rightarrow s$  transition. For the case of  $B^0 \rightarrow \pi^+\pi^-$ , although it is a tree-dominant ( $b \rightarrow u$ ) process, the penguin pollution plays an important role. For illustration, the decay amplitude of  $\bar{B}^0 \rightarrow \pi^+\pi^-$  reads

$$\begin{aligned} \mathcal{A}(\bar{B}^0 \rightarrow \pi^+\pi^-) = & -i\frac{G_F}{\sqrt{2}}f_\pi F^{B\pi}(0)m_B^2\left\{v_u\left[a_1 + a_4^u + a_{10}^u + (a_6^u + a_8^u)r_\chi\right] \right. \\ & \left. + v_c\left[a_4^c + a_{10}^c + (a_6^c + a_8^c)r_\chi\right]\right\}. \end{aligned} \quad (45)$$

Note that  $|v_u| = |V_{ud}^*V_{ub}|$  is at the same order as  $|v_c| = |V_{cd}^*V_{cb}|$  and  $|(a_4 + a_6r_\chi)/a_1| \sim 0.1$ , so the branching ratio of  $\bar{B}^0 \rightarrow \pi^+\pi^-$  is sensitive to both  $|V_{ub}/V_{cb}|$  and  $\gamma = \arg(V_{ub}^*)$ . (In contrast, the decay amplitude of  $B^\pm \rightarrow \pi^0\pi^\pm$  suffers less pollution from the penguin contribution, which is proportional to the small electroweak penguin coefficient  $a_9 + a_{10} - a_7 + a_8r_\chi$ .) Therefore, the variation of  $|V_{ub}/V_{cb}|$  gives large uncertainty to the prediction for the branching ratio of  $B^0 \rightarrow \pi^+\pi^-$ .

All the three modes are dominated by the form factor  $F^{B\pi}(0)$ . Varying  $F^{B\pi}(0)$  from 0.23 to 0.33, it gives about  $\pm 35\%$  uncertainty to the branching ratios. By using the ratios of the branching ratios, the uncertainties caused by the form factor can be largely reduced. This will be shown later.

The endpoint divergence in the hard spectator scattering does not bring large uncertainty to our predictions. The reason is that the endpoint divergence contains only a single logarithmic term and its coefficient is suppressed by  $\alpha_s$  and the color number  $N$ .

Obviously, the endpoint divergence in weak annihilation causes large uncertainty, in particular, to the decays  $B \rightarrow \pi K$ . In Ref. [16], the authors also showed this point. The reason is that the endpoint divergence in weak annihilation is dominated by a product of two logarithmic terms. Within the range of the parameters  $\varrho$  and  $\phi$ , our predictions by the BBNS approach are in agreement with the experimental measurements.

Therefore, we find that weak annihilation is the main source of the uncertainties in the BBNS approach. To obtain a more precise prediction, further analysis is needed of

the weak annihilations. On the other hand, there are other possible power suppressed corrections in the decays  $B \rightarrow PP$ . Some researchers pointed out that the elastic and inelastic long-distance FSI can help us obtain small branching ratio for  $\bar{B}_d^0 \rightarrow \pi^+\pi^-$  at small  $\gamma$  [41,42]. However, with the elastic FSI, in order to get satisfying results, one must introduce a large strong phase difference which is unbelievable in the heavy quark limit. In particular, in Ref. [42], the author takes the inelastic rescattering  $B \rightarrow D\bar{D} \rightarrow \pi\pi$  into account and finds that the small branching ratio of  $\bar{B}_d^0 \rightarrow \pi\pi$  can be obtained at small  $\gamma$  without fine-tuning the input parameters. Furthermore, in Ref. [43], Isola *et al.* give detailed research on the nonperturbative charming penguin effects on  $B \rightarrow \pi K$  and the predictions are in better agreement with the experimental data. However, all treatments to these power corrections are model-dependent. Up to now, there is no systematic way to deal with these complicated nonperturbative interactions. Maybe the precise measurement of the CP asymmetries for the decays  $B \rightarrow PP$  is a chance to distinguish these models.

Here we emphasize that the decay amplitude of  $B^0 \rightarrow K^-K^+$  comes completely from the effects of weak annihilations under the BBNS approach, because contributions of weak annihilations are supposed to be power suppressed, so the CP-averaged branching ratio for  $\bar{B}^0(B^0) \rightarrow K^+K^-$  is small in Fig. 3. At the same time, we can also see that uncertainties of theoretical predictions for these decay modes are very large (the branching ratios range from  $10^{-8}$  to  $10^{-7}$ ). As mentioned above, we expect that we can extract some useful information about the endpoint divergence  $X_A$  from  $B^0 \rightarrow K^+K^-$ . However, the present experimental upper limit is much greater than our predictions within the range of the parameters. If this decay mode can be measured precisely in the future, then we will be able to obtain some useful information on weak annihilations and FSI. Consequently, the endpoint divergence  $X_A$  can be determined effectively.

### C. Ratios of the branching ratios

As mentioned above, the decay rates for  $B \rightarrow PP$  depend on a number of parameters that cannot be predicted with the BBNS approach itself. Thus, these parameters result in ambiguity of the predictions for the CP-averaged branching ratios. In order to reduce uncertainties from the renormalization scale and weak annihilation effects, etc., as much as possible, the ratios of CP-averaged branching ratios are good quantities. Furthermore, many methods have been suggested to give bounds on  $\gamma$  using decay modes of  $B \rightarrow \pi\pi$ ,  $\pi K$ , in which the ratios of branching ratios play important roles. We hope that our calculation can give some constraints on  $\gamma$ . In Fig. 5, we show some ratios of CP-averaged branching ratios versus the weak phase  $\gamma$  (note that we use PDG2000 data for  $\tau_{B^+}/\tau_{B^0} = 1.062$ ), where the slashed-line bands correspond to experimental data listed in Table III with one standard deviation ( $1\sigma$ ).

Obviously, using the ratios of branching ratios, and comparing with Fig. 3, the width of dot-shades becomes narrow due to the reduction of the uncertainty. From Fig. 5(b), the ratio  $\text{BR}(B^0 \rightarrow \pi^\mp K^\pm)/(2\text{BR}(B^0 \rightarrow \pi^0 K^0))$  can be made consistent with the experimental data at small  $\gamma$ . However, the ratio  $\tau_{B^+}/\tau_{B^0}[\text{BR}(B^0 \rightarrow \pi^+\pi^-)/(2\text{BR}(B^0 \rightarrow \pi^\pm\pi^0))]$  tends to be consistent with the experimental data at large  $\gamma$  in Fig. 5(e). Considering the correlation between these quantities, a scientific choice is to give a global fit for these branching ratios and/or the ratios of the branching ratios. In Ref. [16], the authors give a

global fit for  $(\bar{\rho}, \bar{\eta})$  from  $B$  rare hadronic decays with the QCD factorization. The result favors large  $\gamma$  (about  $90^\circ$ ) and/or small  $|V_{ub}|$  [16,36,37].

There are many discussions on ratios of branching ratios, for instance in [11,12], in order to determine coefficients  $a_i$ , and extract the CKM matrix parameters, etc. In particular, the decay modes  $B \rightarrow K\pi$  are widely discussed to get information on  $\gamma$ ; readers interested in these topics are referred to, for instance, [44,45]. From Figs. 5(a) and 5(b), our theoretical results show that

$$\frac{2\text{BR}(B^\pm \rightarrow \pi^0 K^\pm)}{\text{BR}(B^\pm \rightarrow \pi^\pm K^0)} \approx \frac{\text{BR}(B^0 \rightarrow \pi^\mp K^\pm)}{2\text{BR}(B^0 \rightarrow \pi^0 K^0)} \quad (46)$$

This approximate relation can also be obtained from the isospin decomposition of the effective Hamiltonian <sup>4</sup> [46]. The experimental data listed in Table III give

$$\frac{2\text{BR}(\pi^0 K^\pm)}{\text{BR}(\pi^\pm K^0)} = 1.18 \pm 0.34 (\text{BaBar}), \quad \frac{\text{BR}(\pi^\mp K^\pm)}{2\text{BR}(\pi^0 K^0)} = 1.02 \pm 0.41 (\text{BaBar}), \quad (47)$$

which are consistent with Eq.(46).

#### D. CP-violating asymmetries

CP violation in  $B$  meson decays can be either direct or indirect. Typically, direct CP-violating asymmetry arises when the tree and penguin amplitudes interfere. CP violations in decays of charged  $B$  meson are purely direct; as these decays are all self-tagging, they are the definitive signals of CP violation if seen. The direct CP-violating symmetry is defined by

$$\mathcal{A}_{CP} = \frac{\Gamma(B^- \rightarrow f^-) - \Gamma(B^+ \rightarrow f^+)}{\Gamma(B^- \rightarrow f^-) + \Gamma(B^+ \rightarrow f^+)}. \quad (48)$$

Because the flavor eigenstates  $\bar{B}^0$  and  $B^0$  mix due to weak interactions, direct and indirect CP violation occur simultaneously in neutral  $B$  meson decays, and time-dependent measurements of CP-violating asymmetries are needed.

$$\mathcal{A}_{CP}(t) = \frac{\Gamma(\bar{B}^0(t) \rightarrow \bar{f}) - \Gamma(B^0(t) \rightarrow f)}{\Gamma(\bar{B}^0(t) \rightarrow \bar{f}) + \Gamma(B^0(t) \rightarrow f)}. \quad (49)$$

For  $B^0 \rightarrow f$  (but  $B^0 \not\rightarrow \bar{f}$ ) and  $\bar{B}^0 \rightarrow \bar{f}$  (but  $\bar{B}^0 \not\rightarrow f$ ), the CP-violating asymmetries are similar to those of charged  $B$  mesons. For  $\bar{B}^0 \rightarrow (\bar{f} = f, CP|f) \leftarrow B^0$ , i.e., the final states are CP eigenstates, the time-integrated CP-violating asymmetries are:

---

<sup>4</sup>In Ref. [46], the isospin amplitudes are defined as  $B_{1/2} = \sqrt{2/3}\langle 1/2, \pm 1/2 | \mathcal{H}_{\Delta I=0} | 1/2, \pm 1/2 \rangle$ , which arises from QCD penguin operators, while  $A_{1/2} = \pm \sqrt{2/3}\langle 1/2, \pm 1/2 | \mathcal{H}_{\Delta I=1} | 1/2, \pm 1/2 \rangle$ ,  $A_{3/2} = \sqrt{1/3}\langle 3/2, \pm 1/2 | \mathcal{H}_{\Delta I=1} | 1/2, \pm 1/2 \rangle$ , which include contributions from tree and electroweak operators. Moreover,  $|B_{1/2}| \approx \mathcal{O}(10^{-3})$ ,  $|A_{1/2}| \approx \mathcal{O}(10^{-5})$ , and  $|A_{3/2}| \approx \mathcal{O}(10^{-4})$ . The decay amplitudes can be described as  $\mathcal{A}(B^+ \rightarrow \pi^+ K^0) = A_{3/2} + A_{1/2} + B_{1/2}$ , and  $\sqrt{2}\mathcal{A}(B^+ \rightarrow \pi^0 K^+) = 2A_{3/2} - A_{1/2} - B_{1/2}$ . Neglecting effects of  $A_{3/2}$  and  $A_{1/2}$ , we can get a good approximation to Eq.(46).

$$\mathcal{A}_{CP} = \frac{1}{1+x^2}a_{e'} + \frac{x}{1+x^2}a_{\epsilon+\epsilon'}, \quad (50)$$

$$a_{e'} = \frac{1-|\lambda_f|^2}{1+|\lambda_f|^2}, \quad a_{\epsilon+\epsilon'} = \frac{-2\text{Im}(\lambda_f)}{1+|\lambda_f|^2}, \quad \lambda_f = \frac{V_{tb}^*V_{td}\langle f|\mathcal{H}_{eff}|\overline{B}^0\rangle}{V_{tb}V_{td}^*\langle f|\mathcal{H}_{eff}|B^0\rangle}, \quad (51)$$

with the PDG2000 data value  $x = \Delta m/\Gamma = 0.73 \pm 0.03$  for  $B^0-\overline{B}^0$  system. Here  $a_{e'}$  and  $a_{\epsilon+\epsilon'}$  are due to direct and mixing-induced CP violation, respectively.

Recent experimental measurements of CP-violating asymmetries  $\mathcal{A}_{CP}$  for  $B \rightarrow \pi K$ ,  $K\eta'$  and  $a_{e'}$ ,  $a_{\epsilon+\epsilon'}$  for  $\overline{B}_d^0 \rightarrow \pi^+\pi^-$  are listed in Table V. These results contain very large errors and they are consistent with zero. Precise measurements of direct CP violation and time-dependent CP violation are expected in the near future.

Theoretically, CP-violating asymmetries will not be very large in the BBNS approach in principle, because the strong phases are suppressed by  $\alpha_s$  or  $\Lambda_{QCD}/m_b$ . However, from Table II we know that  $a_{2,4,6}$  have large imaginary parts. When they are dominant in some decay modes, large CP violations are expected, for instance, in  $\overline{B}^0(B^0) \rightarrow \pi^0\pi^0$ ,  $\pi^0\eta^{(\prime)}$ ,  $\eta^{(\prime)}\eta^{(\prime)}$ .

With the BBNS approach, CP-violating asymmetries depend on several variables, such as the form factors, CKM parameters, the scale  $\mu$ , and so on. Our investigation indicates that CP-violating asymmetries for all  $B \rightarrow PP$  depend very weakly on form factors; the same conclusion can be obtained with the GF approach. So we show results only with the default values of the form factors in the following calculations. As for the dependence of CP-violating asymmetries on scale  $\mu$ , there are six decay modes  $\overline{B}^0(B^0) \rightarrow \pi^0\pi^0$ ,  $\pi^0\eta^{(\prime)}$ ,  $\eta^{(\prime)}\eta^{(\prime)}$  to be singled out because they are strongly  $\mu$  dependent compared with other decay modes. In these six decay modes,  $a_2$  is involved and not CKM-suppressed, and it is sensitive to the renormalization scale. This point has been shown in Table II. In particular, its imaginary part is larger than the real part, which might result in large CP violations in these decay modes as we show in Table VI. We also list CP-violating asymmetries versus the weak phase  $\gamma$  in Table VII and Table VIII. The endpoint divergence can cause large theoretical uncertainties; its influence on CP-violating asymmetries is shown in Table IX.

From Table VI to Table IX, we can clearly see that theoretical predictions on CP-violating asymmetries are compatible with measurements within one standard deviation ( $1\sigma$ ). Unfortunately, the present experimental uncertainties are too large to draw any meaningful conclusion. In addition, the weak annihilations have great influence on CP-violating asymmetries, so their contributions to decay amplitudes must be included in estimation of CP violation in  $B$  meson decays with the BBNS approach. Moreover, the power corrections in order of  $\Lambda_{QCD}/m_b$  which are not included in the QCDF master formula (5). This needs further investigation.

Here we would like to point out that  $B \rightarrow \pi\pi$  are usually considered to determine the CKM angles  $\alpha$  and  $\gamma$  using CP-violating asymmetry [47,48]. From Table VII and Table VIII, we can see that  $\mathcal{A}(\pi^+\pi^-)$ , especially the mixing-induced  $a_{\epsilon+\epsilon'}$  (%) term, are sensitive to the CKM angle  $\gamma$ . This mode is strongly polluted by the penguins. As to the large penguin pollution, recently, Fleischer suggested a new approach [47]. Using U-spin SU(3) flavour symmetry,  $B_d \rightarrow \pi^+\pi^-$  and  $B_s \rightarrow K^+K^-$  are related to each other by interchanging the  $d$  quark and  $s$  quark, which possibly allows a simultaneous determination  $\beta$  and  $\gamma$ . His analysis gives  $\gamma = 76^\circ$  and  $\phi_d = 2\beta = 53^\circ$  without considering the U-spin-breaking effects.

As we see from Table VII and Table VIII, time-integrated CP-violating asymmetries  $\mathcal{A}_{CP}$  for  $\overline{B}^0 \rightarrow K_S^0 \pi$ ,  $K_S^0 \eta^{(\prime)}$  are completely dominated by mixing-induced  $a_{\epsilon+\epsilon'}$  term. But we still do not know the  $\eta^{(\prime)}$  production mechanism. Hence it is useless to discuss the CP-violating asymmetries  $\mathcal{A}_{CP}(K_S^0 \eta^{(\prime)})$ . As to CP-violating asymmetries for  $\overline{B}^0 \rightarrow K^+ K^-$ , they do not contain the direct CP-violating  $a'_\epsilon$  term, and arise only from  $a_{\epsilon+\epsilon'}$  term. Moreover, they are sensitive to the CKM angle  $\gamma$ . However, we know that with the BBNS approach the branching ratios for neutral  $B$  meson decays into  $K^+ K^-$  have only weak annihilations contributions, which are scale  $\mu$  dependent and contain large theoretical uncertainties due to their soft nonperturbative effects.

## V. CONCLUSIONS

(1) In the heavy quark limit, neglecting the effects of order  $\Lambda_{QCD}/m_b$ , the contributions that are non-factorizable under the GF framework can be factorized with the BBNS approach, and they are perturbatively calculable from first principles, at least at order of  $\alpha_s$ . The BBNS approach provides decay amplitudes with strong phases which are usually small, at order of  $\alpha_s$  and/or  $\Lambda_{QCD}/m_b$ .

(2) CP-averaged branching ratios of  $B \rightarrow PP$  in the BBNS approach are less renormalization scale dependent than those under the NF framework, especially when the chirally enhanced corrections are taken into account; generally, with the appropriate parameters, predictions with the BBNS approach are consistent with present experimental data. However, the theoretical predictions include very large uncertainties which arise from various parameters, such as the form factors, CKM matrix elements and soft endpoint divergence, etc. Our results show that the theoretical uncertainties from the endpoint divergence  $X_A$  are considerable. Likewise, CP-violating asymmetries for  $B \rightarrow PP$  in the BBNS approach are also sensitive to variation of endpoint divergences. In particular, decay amplitudes for  $\overline{B}^0(B^0) \rightarrow K^+ K^-$  arise completely from weak annihilations with the BBNS approach; we can obtain very useful information on the effects of FSI and soft weak annihilations with precise experimental data in the future.

(3) The present experimental data for non-leptonic  $B$  meson decays are not precise enough yet, especially for the measurements of CP violation. On the other hand, there are still many uncertainties in the theoretical framework, for instance, the hard spectator scattering, weak annihilations and other potential power corrections. Great advances in both experiment and theory in the near future are expected to determine the CKM angles precisely.

## ACKNOWLEDGEMENTS

This work is Supported in part by National Natural Science Foundation of China. We thank Profs. Zhi-zhong Xing and Mao-Zhi Yang for helpful discussions.

## APPENDIX: THE ANNIHILATION AMPLITUDES FOR $B \rightarrow PP$

$$A^{ann}(\overline{B}^0 \rightarrow \pi^+ \pi^-) = -i \frac{G_F}{\sqrt{2}} f_B f_\pi^2 \left[ v_u b_1 + (v_u + v_c) \left( b_3 + 2b_4 - \frac{1}{2} b_3^{ew} + \frac{1}{2} b_4^{ew} \right) \right], \quad (A1)$$

$$A^{ann}(\overline{B}^0 \rightarrow \pi^0 \pi^0) = A^{ann}(\overline{B}^0 \rightarrow \pi^+ \pi^-), \quad (\text{A2})$$

$$A^{ann}(B^- \rightarrow \pi^0 \pi^-) = 0, \quad (\text{A3})$$

$$A^{ann}(\overline{B}^0 \rightarrow \pi^0 \overline{K}^0) = i \frac{G_F}{2} f_B f_\pi f_K \left[ (v_u + v_c) (b_3 - \frac{1}{2} b_3^{ew}) \right], \quad (\text{A4})$$

$$A^{ann}(\overline{B}^0 \rightarrow \pi^+ K^-) = -\sqrt{2} A^{ann}(\overline{B}^0 \rightarrow \pi^0 \overline{K}^0), \quad (\text{A5})$$

$$A^{ann}(B^- \rightarrow \pi^0 K^-) = -i \frac{G_F}{2} f_B f_\pi f_K \left[ v_u b_2 + (v_u + v_c) (b_3 + b_3^{ew}) \right], \quad (\text{A6})$$

$$A^{ann}(B^- \rightarrow \pi^- \overline{K}^0) = \sqrt{2} A^{ann}(B^- \rightarrow \pi^0 K^-), \quad (\text{A7})$$

$$A^{ann}(\overline{B}^0 \rightarrow \pi^0 \eta^{(\prime)}) = -i \frac{G_F}{2} f_B f_\pi f_{\eta^{(\prime)}}^u \left[ v_u 2b_1 + (v_u + v_c) (-2b_3 + b_3^{ew} + 3b_4^{ew}) \right], \quad (\text{A8})$$

$$A^{ann}(B^- \rightarrow \pi^- \eta^{(\prime)}) = -i \frac{G_F}{\sqrt{2}} f_B f_\pi f_{\eta^{(\prime)}}^u \left[ v_u 2b_2 + (v_u + v_c) (2b_3 + 2b_3^{ew}) \right], \quad (\text{A9})$$

$$A^{ann}(\overline{B}^0 \rightarrow \eta^{(\prime)} \eta^{(\prime)}) = -i \frac{G_F}{\sqrt{2}} f_B f_{\eta^{(\prime)}}^u{}^2 \left[ v_u 2b_1 + (v_u + v_c) (2b_3 + 4b_4 - b_3^{ew} + b_4^{ew}) \right. \\ \left. + (v_u + v_c) \left( \frac{f_{\eta^{(\prime)}}^s}{f_{\eta^{(\prime)}}^u} \right)^2 (2b_4 - b_4^{ew}) \right], \quad (\text{A10})$$

$$A^{ann}(\overline{B}^0 \rightarrow \eta \eta^{(\prime)}) = -i \frac{G_F}{\sqrt{2}} f_B f_\eta^u f_{\eta^{(\prime)}}^u \left[ v_u 2b_1 + (v_u + v_c) (2b_3 + 4b_4 - b_3^{ew} + b_4^{ew}) \right. \\ \left. + (v_u + v_c) \frac{f_{\eta^{(\prime)}}^s f_\eta^s}{f_{\eta^{(\prime)}}^u f_\eta^u} (2b_4 - b_4^{ew}) \right], \quad (\text{A11})$$

$$A^{ann}(B^- \rightarrow K^- \eta^{(\prime)}) = -i \frac{G_F}{\sqrt{2}} f_B f_K f_{\eta^{(\prime)}}^u \left( 1 + \frac{f_{\eta^{(\prime)}}^s}{f_{\eta^{(\prime)}}^u} \right) \left[ v_u b_2 + (v_u + v_c) (b_3 + b_3^{ew}) \right], \quad (\text{A12})$$

$$A^{ann}(\overline{B}^0 \rightarrow \overline{K}^0 \eta^{(\prime)}) = -i \frac{G_F}{\sqrt{2}} f_B f_K f_{\eta^{(\prime)}}^u \left( 1 + \frac{f_{\eta^{(\prime)}}^s}{f_{\eta^{(\prime)}}^u} \right) \left[ (v_u + v_c) (b_3 - \frac{1}{2} b_3^{ew}) \right], \quad (\text{A13})$$

$$A^{ann}(\overline{B}^0 \rightarrow \overline{K}^0 K^0) = -i \frac{G_F}{\sqrt{2}} f_B f_K^2 \left[ (v_u + v_c) (b_3 + 2b_4 - \frac{1}{2} b_3^{ew} - b_4^{ew}) \right], \quad (\text{A14})$$

$$A^{ann}(B^- \rightarrow K^- K^0) = -i \frac{G_F}{\sqrt{2}} f_B f_K^2 \left[ v_u b_2 + (v_u + v_c) (b_3 + b_3^{ew}) \right], \quad (\text{A15})$$

$$A^{ann}(\overline{B}^0 \rightarrow K^+ K^-) = -i \frac{G_F}{\sqrt{2}} f_B f_K^2 \left[ v_u b_1 + (v_u + v_c) (2b_4 + \frac{1}{2} b_4^{ew}) \right], \quad (\text{A16})$$

The annihilation coefficients  $(b_1, b_2)$ ,  $(b_3, b_4)$  and  $(b_3^{ew}, b_4^{ew})$  correspond to the contributions from tree, QCD penguins and electroweak penguins operators, respectively. They are related to final state mesons. Using the asymptotic light cone distribution amplitudes of the mesons, and assuming  $SU(3)$  flavor symmetry, they can be expressed as [16]

$$b_1 = \frac{C_F}{N_c^2} C_1 A^i, \quad b_3 = \frac{C_F}{N_c^2} \left[ C_3 A^i + A^f (C_5 + N_c C_6) \right], \quad (\text{A17})$$

$$b_2 = \frac{C_F}{N_c^2} C_2 A^i, \quad b_4 = \frac{C_F}{N_c^2} A^i (C_4 + C_6), \quad (\text{A18})$$

$$b_3^{ew} = \frac{C_F}{N_c^2} \left[ C_9 A^i + A^f (C_7 + N_c C_8) \right], \quad (\text{A19})$$

$$b_4^{ew} = \frac{C_F}{N_c^2} A^i (C_{10} + C_8), \quad (\text{A20})$$

and

$$A^i \approx \pi \alpha_s \left[ 18 \left( X_A - 4 + \frac{\pi^2}{3} \right) + 2r_\chi^2 X_A^2 \right] \quad (\text{A21})$$

$$A^f \approx 12\pi \alpha_s r_\chi (2X_A^2 - X_A), \quad (\text{A22})$$

where  $X_A = \int_0^1 \mathbf{d}\mathbf{y}/y$  is a logarithmically divergent integral, and will be phenomenologically parameterized in the calculation.

## REFERENCES

- [1] CLEO Collaboration, D. Cronin-Hennessy *et al.*, Phys. Rev. Lett. **85** 515 (2000); CLEO Collaboration, S. Chen *et al.*, *ibid.* **85** 525 (2000); CLEO Collaboration, S.J. Richichi *et al.*, *ibid.* **85** 520 (2000).
- [2] Babar Collaboration, G. Cavoto, hep-ex/0105018; Babar Collaboration, B. Aubert *et al.*, Phys. Rev. Lett. **87**, 151802 (2001); hep-ex/0107074, hep-ex/0108017; Babar Collaboration, J. Olsen, hep-ex/0011031.
- [3] Belle Collaboration, T. Iijima, hep-ex/0105005; Belle Collaboration, K. Abe *et al.*, Phys. Rev. Lett. **87**, 101801, (2001); Phys. Rev. **D64**, 071101, (2001); Phys. Lett. **B517**, 309 (2001).
- [4] For a review, see G. Buchalla, A.J. Buras and M.E. Lautenbacher, Rev. Mod. Phys. **68** 1125 (1996) ; or A.J. Buras, hep-ph/9806471.
- [5] M. Bauer and B. Stech, Phys. Lett. **B152** 380 (1985); M.Bauer, B.Stech and M.Wirbel, Z. Phys. **C34** (1987) 103.
- [6] J.D. Bjorken, Nucl. Phys. B(Proc. Suppl.) **11**, 325 (1989).
- [7] H.Y. Cheng, Phys. Lett. **B335** 428 (1994); **B395** 345 (1997); H.Y. Cheng and B. Tseng, Phys. Rev. **D58** 094005 (1998); A. Ali and C. Greub, *ibid.* **57** 2996 (1998); A. Ali, J. Chay, C. Greub and P. Ko, Phys. Lett. **B424** 161 (1998); M. Neubert, Nucl. Phys. B (Proc.Suppl.) **64** 474 (1998); J. M. Soares, Phys. Rev. **D51** 3518 (1995).
- [8] APE Collaboration, A. Abada *et al.*, Phys. Lett. **B365**, 275 (1996); J.M. Flynn and C.T. Sachrajda, *Heavy flavours II*, pp. 402-452, (hep-lat/9710057); UKQCD Collaboration, J.M. Flynn *et al.*, Nucl. Phys. **B461**, 327 (1996); UKQCD Collaboration, L. Del Debbio *et al.*, Phys. Lett. **B416**, 392 (1998).
- [9] P. Ball and V.M. Braun, Phys. Rev. **D55**, 5561, (1997); J. High Energy Phys. **09**, 005, (1998).
- [10] A. Khodjamirian, R. Rückl, S. Weinzierl and O. Yakovlev, Phys. Lett. **B410**, 275 (1997); A. Khodjamirian, R. Rückl and C.W. Winhart, Phys. Rev. **D58**, 054013 (1998); A. Khodjamirian, R. Rückl, *Heavy flavours II*, pp. 345-401, hep-ph/9801443; A. Khodjamirian, R. Rückl, S. Weinzierl, C.W. Winhart, O. Yakovlev, Phys. Rev. **D62**, 114002 (2000)
- [11] A. Ali, G. Kramer and C.D. Lü, Phys. Rev. **D58** 094009 (1998); **59** 014005 (1999).
- [12] Y.H. Chen, H.Y. Cheng, B. Tseng and K.C. Yang, Phys. Rev. **D60**, 094014 (1999).
- [13] M. Beneke, G. Buchalla, M. Neubert and C.T. Sachrajda, Phys. Rev. Lett. **83**, 1914 (1999).
- [14] M. Beneke, G. Buchalla, M. Neubert and C.T. Sachrajda, hep-ph/0007256.
- [15] D.S. Du, D.S. Yang and G.H. Zhu, hep-ph/0008216; Phys. Lett. **B509**, 263 (2001); Phys. Rev. **D64**, 014036 (2001).
- [16] M. Beneke, G. Buchalla, M. Neubert and C.T. Sachrajda, Nucl. Phys. **B606**, 245 (2001).
- [17] J. Chay, Phys.Lett. **B476**, 339 (2000).
- [18] M. Beneke, G. Buchalla, M. Neubert and C.T. Sachrajda, Nucl. Phys. **B591**, 313 (2000).
- [19] D.S. Du, D.S. Yang and G.H. Zhu, Phys. Lett. **B488**, 46 (2000).
- [20] T. Muta, A. Sugamoto, M.Z. Yang and Y.D. Yang, Phys. Rev. **D62**, 094020 (2000).
- [21] M.Z. Yang and Y.D. Yang, Phys. Rev. **D62**, 114019 (2000); Nucl. Phys. **B609**, 469 (2001).
- [22] X.G. He, J.P. Ma and C.Y. Wu, Phys. Rev. **D63**, 094004 (2001).



- [23] J. Chay, C. Kim, hep-ph/0009244.
- [24] H.Y. Cheng and K.C. Yang, Phys. Rev. **D63**, 074011, (2001); **64**, 074004 (2001).
- [25] Y.Y. Keum, H.N. Li, A.I. Sanda, Phys. Rev. **D63**, 054008 (2001); Phys. Lett. **B504**, 6 (2001).
- [26] S. Descotes-Genon and C.T. Sachrajda, hep-ph/0109260.
- [27] M. Bander, D. Silverman and A. Soni, Phys. Rev. Lett. **43**, 242 (1979).
- [28] V.L. Chernyak and A.R. Zhitnitsky, Phys. Rep. **112**, 173 (1983); V.M. Braun and I.B. Filyanov, Z. Phys. **C48**, 239 (1990); P. Ball, J. High Energy Phys. **01**, 010 (1999).
- [29] M. Beneke, J. Phys. **G27**, 1069 (2001).
- [30] D.S. Du, C.S. Huang, Z.T. Wei and M.Z. Yang, Phys. Lett. **B520**, 50 (2001).
- [31] H.N. Li, hep-ph/0103305; T. Kurimoto, H.N. Li and A. I. Sanda, Phys. Rev. **D65**, 014007 (2002).
- [32] C.D. Lü, K. Ukai and M.Z. Yang, Phys.Rev. **D63**, 074009 (2001).
- [33] M.Ciuchini *et al.*, J. High Energy Phys. **07**, 13 (2001).
- [34] T. Feldmann, P. Kroll, B. Stech, Phys. Rev. **D58**, 114006 (1998).
- [35] P. Colangelo and A. Khodjamirian, in *At the Frontier of Particle Physics / Handbook of QCD*, Boris Ioffe Festschrift, edited by M. Shifman (World Scientific, Singapore, in press), hep-ph/0010175.
- [36] M. Neubert, talk given in the XXth International Symposium on Lepton and Photon Interactions at High Energies, Roma, Italy, 2001, hep-ph/0110301.
- [37] M. Neubert, talk presented at the International Workshop on QCD: Theory and Experiment, Martina Franca, Italy, 2001, and at the 9th International Symposium on Heavy Flavour Physics, Pasadena, CA, 2001, hep-ph/0110093.
- [38] D.S. Du, C.S. Kim and Y.D. Yang, Phys. Lett. **B426**, 133 (1998); A.L. Kagan and A.A. Petrov, hep-ph/9707354; A.L. Kagan, hep-ph/9806266; M.R. Ahmady, E. Kou and A. Sugamoto, Phys. Rev. **D58**, 014015 (1998).
- [39] D.S. Du, D.S. Yang and G.H. Zhu, HEP & NP, **26(1)**, 1-7 (2002)(in Chinese), hep-ph/9912201.
- [40] C.H. Chen, H.N. Li, Phys. Rev. **D63**, 014003 (2001).
- [41] W.S. Hou and K.C. Yang, Phys. Rev. Lett. **84**, 4806 (2000).
- [42] Z.Z. Xing, Phys. Lett. **B493**, 301 (2000).
- [43] C. Isola *et al.*, Phys. Rev. **D64**, 014029 (2001); hep-ph/0110411.
- [44] M. Neubert and J.R. Rosner, Phys. Lett. **B441**, 403 (1998).
- [45] R. Fleischer and T. Mannel, Phys. Rev. **D57**, 2752 (1998); A.J. Buras and R. Fleischer, Eur. Phys. J. **C16**, 97 (2000).
- [46] M. Neubert, Phys. Lett. **B424**, 152 (1998);
- [47] R. Fleischer, Eur. Phys. J **C16**, 87 (2000); hep-ph/0011323.
- [48] I.I. Bigi and A.I. Sanda, Nucl. Phys. **B281**, 41 (1987); Y. Nir and H.R. Quinn, Ann. Rev. Nucl. Part. Sci. **42**, 211 (1992); P.Ball, hep-ph/0010024.

TABLES

TABLE I. Wilson coefficients in NDR scheme. The input parameters in numerical calculation are fixed:  $\alpha_s(m_Z) = 0.1185$ ,  $\alpha_{em}(m_W) = 1/128$ ,  $m_W = 80.42\text{GeV}$ ,  $m_Z = 91.188\text{GeV}$ ,  $m_t = 168.2\text{GeV}$ ,  $m_b = 4.6\text{GeV}$ .

	$\mu = m_b/2$	$\mu = m_b$	$\mu = 2m_b$
$C_1$	1.136	1.080	1.044
$C_2$	-0.283	-0.181	-0.105
$C_3$	0.021	0.014	0.009
$C_4$	-0.050	-0.035	-0.024
$C_5$	0.010	0.009	0.007
$C_6$	-0.063	-0.041	-0.026
$C_7/\alpha_{em}$	-0.020	-0.004	0.019
$C_8/\alpha_{em}$	0.082	0.052	0.033
$C_9/\alpha_{em}$	-1.339	-1.263	-1.201
$C_{10}/\alpha_{em}$	0.369	0.253	0.168
$C_{7\gamma}$	-0.341	-0.304	-0.272
$C_{8g}$	-0.160	-0.145	-0.132

TABLE II. Numerical values of coefficients  $a_i$  with  $m_b = 4.6\text{GeV}$ ,  $m_c = 1.45\text{GeV}$  and  $f^{II} = 0$ .

	$\mu = m_b/2$	$\mu = m_b$	$\mu = 2m_b$
$a_1^u$	1.070+0.026i	1.046+0.013i	1.027+0.006i
$a_2^u$	-0.019-0.106i	0.023-0.079i	0.062-0.064i
$a_3(10^{-4})$	93.662+46.585i	73.837+25.729i	51.675+14.646i
$a_4^u(10^{-4})$	-330.78-179.23i	-297.17 -146.84i	-267.83 -125.46i
$a_4^c(10^{-4})$	-403.19-55.903i	-351.48-54.337i	-311.41 -51.226i
$a_5(10^{-4})$	-98.679-58.697i	-67.453-30.139i	-41.612 -15.867i
$a_6^u(10^{-4})$	-556.39-159.84i	-411.61-136.65i	-322.84 -120.02i
$a_6^c(10^{-4})$	-597.2-34.652i	-442.22-42.742i	-347.41 -44.663i
$a_6^u r_\chi(10^{-4})$	-474.17-136.22i	-469.29-155.8 i	-459.82-170.95i
$a_6^c r_\chi(10^{-4})$	-508.95-29.531i	-504.19-48.731i	-494.81-63.614i
$a_7(10^{-4})$	0.458+0.597i	1.248+0.299i	2.591+0.157i
$a_8^u(10^{-4})$	6.980-0.66i	4.255-1.117i	2.336-1.465i
$a_8^c(10^{-4})$	6.884-0.365i	4.076-0.566i	2.092-0.717i
$a_8^u r_\chi(10^{-4})$	5.949-0.562i	4.852-1.274i	3.328-2.087i
$a_8^c r_\chi(10^{-4})$	5.867-0.311i	4.647-0.645i	2.980-1.021i
$a_9(10^{-4})$	-97.902-2.686i	-94.935-1.453i	-91.732-0.801i
$a_{10}^u(10^{-4})$	7.414+9.087i	3.136+6.136i	-0.956+4.261i
$a_{10}^c(10^{-4})$	7.244+9.377i	2.817+6.679i	-1.389+4.998i

TABLE III. Experimental data of CP-averaged branching ratios for  $B \rightarrow \pi\pi$ ,  $\pi K$ ,  $K\eta'$  in unit of  $10^{-6}$ .

Decay Modes	CLEO [1]	BaBar [2]	Belle [3]
$\overline{B}^0 \rightarrow \pi^+ \pi^-$	$4.3_{-1.4}^{+1.6} \pm 0.5$	$4.1 \pm 1.0 \pm 0.7$	$5.6_{-2.0}^{+2.3} \pm 0.4$
$B^\pm \rightarrow \pi^\pm \pi^0$	$5.6_{-2.3}^{+2.6} \pm 1.7$	$5.1_{-1.8}^{+2.0} \pm 0.8$	$7.8_{-3.2}^{+3.8} \pm 0.8$
$\overline{B}^0 \rightarrow \pi^\pm K^\mp$	$17.2_{-2.4}^{+2.5} \pm 1.2$	$16.7 \pm 1.6 \pm 1.3$	$19.3_{-3.2}^{+3.4} \pm 1.5$
$B^\pm \rightarrow \pi^0 K^\pm$	$11.6_{-2.7}^{+3.0} \pm 1.4$	$10.8_{-1.9}^{+2.1} \pm 1.0$	$16.3_{-3.3}^{+3.5} \pm 1.6$
$B^\pm \rightarrow \pi^\pm K^0$	$18.2_{-4.0}^{+4.6} \pm 1.6$	$18.2_{-3.0}^{+3.3} \pm 1.7$	$13.7_{-4.8}^{+5.7} \pm 1.9$
$\overline{B}^0 \rightarrow \pi^0 \overline{K}^0$	$14.6_{-5.1}^{+5.9} \pm 2.4$	$8.2_{-2.7}^{+3.1} \pm 1.1$	$16.0_{-5.9}^{+7.2} \pm 2.5$
$B^- \rightarrow K^- \eta'$	$80_{-9}^{+10} \pm 7$	$70 \pm 8 \pm 5$	$79_{-11}^{+12} \pm 9$
$\overline{B}^0 \rightarrow \overline{K}^0 \eta'$	$89_{-16}^{+18} \pm 9$	$42_{-11}^{+13} \pm 4$	$55_{-16}^{+19} \pm 8$

TABLE IV. Numerical predictions for CP-averaged branching ratios (in unit of  $10^{-6}$ ) for  $B \rightarrow PP$ , in the framework of NF and QCDF, where  $\text{BR}^f$  and  $\text{BR}^{f+a}$  denote the CP-averaged branching ratios without and with the contributions from weak annihilation, respectively. The experimental data is from PDG2000; \* denotes uncorrelated averages of Table III.

Decay Modes	$\mu = m_b/2$			$\mu = m_b$			$\mu = 2m_b$			Exp.
	NF	QCDF		NF	QCDF		NF	QCDF		
	BR	$\text{BR}^f$	$\text{BR}^{f+a}$	BR	$\text{BR}^f$	$\text{BR}^{f+a}$	BR	$\text{BR}^f$	$\text{BR}^{f+a}$	
$\overline{B}^0 \rightarrow \pi^+ \pi^-$	9.74	10.06	10.49	9.09	9.67	9.97	8.68	9.36	9.58	$4.4 \pm 0.9^*$
$B^- \rightarrow \pi^- \pi^0$	5.58	5.26	—	6.20	5.36	—	6.76	5.52	—	$5.7 \pm 1.5^*$
$B^- \rightarrow \pi^- \eta$	3.41	3.27	3.22	3.59	3.28	3.26	3.74	3.34	3.33	$< 15$
$B^- \rightarrow \pi^- \eta'$	2.26	2.23	2.18	2.53	2.26	2.24	2.71	2.35	2.34	$< 12$ [3]
$\overline{B}^0 \rightarrow \pi^0 \eta$	0.17	0.17	0.18	0.12	0.15	0.16	0.07	0.14	0.15	$< 8$
$\overline{B}^0 \rightarrow \pi^0 \eta'$	0.038	0.048	0.054	0.037	0.045	0.053	0.026	0.049	0.057	$< 11$
$\overline{B}^0 \rightarrow \pi^0 \pi^0$	0.12	0.11	0.18	0.15	0.099	0.13	0.23	0.10	0.12	$< 9.3$
$\overline{B}^0 \rightarrow \eta \eta$	0.077	0.078	0.104	0.095	0.076	0.093	0.12	0.081	0.093	$< 18$
$\overline{B}^0 \rightarrow \eta' \eta'$	0.009	0.016	0.022	0.029	0.015	0.022	0.048	0.021	0.027	$< 47$
$\overline{B}^0 \rightarrow \eta \eta'$	0.059	0.073	0.066	0.11	0.073	0.073	0.15	0.086	0.09	$< 27$
$\overline{B}^0 \rightarrow K^- \pi^+$	10.66	9.56	10.45	6.40	8.59	9.13	3.4	7.78	8.09	$17.4 \pm 1.5^*$
$\overline{B}^0 \rightarrow \overline{K}^0 \pi^0$	4.99	4.52	4.96	2.90	4.01	4.27	1.44	3.57	3.72	$10.3 \pm 2.6^*$
$B^- \rightarrow K^- \pi^0$	7.65	7.04	7.56	4.83	6.36	6.67	2.82	5.78	5.96	$12.1 \pm 1.6^*$
$B^- \rightarrow \overline{K}^0 \pi^-$	14.43	13.45	14.48	8.8	11.99	12.61	4.79	10.72	11.08	$17.3 \pm 2.5^*$
$B^- \rightarrow K^- \eta$	2.91	2.67	2.78	1.68	2.31	2.37	0.94	1.96	2.0	$< 14$
$B^- \rightarrow K^- \eta'$	16.6	16.72	17.82	12.47	15.74	16.87	7.49	15.75	16.55	$74.9 \pm 6.6^*$
$\overline{B}^0 \rightarrow \overline{K}^0 \eta$	1.93	1.70	1.79	1.0	1.45	1.50	0.45	1.21	1.24	$< 33$
$\overline{B}^0 \rightarrow \overline{K}^0 \eta'$	17.07	17.33	18.13	12.82	16.26	17.12	7.79	16.14	16.73	$59.6 \pm 9.8^*$
$B^- \rightarrow K^- K^0$	0.78	0.75	0.79	0.47	0.67	0.69	0.26	0.59	0.61	$< 2.5$ [2]
$\overline{B}^0 \rightarrow \overline{K}^0 K^0$	0.73	0.71	0.84	0.44	0.62	0.70	0.24	0.56	0.60	$< 17$
$\overline{B}^0 \rightarrow K^+ K^-$	—	—	0.044	—	—	0.033	—	—	0.03	$< 2.5$ [2]

TABLE V. Experimental data of CP-violating asymmetries  $\mathcal{A}_{CP}$  for  $B \rightarrow \pi K, K\eta'$ ,  $a_{\epsilon'}$ , and  $a_{\epsilon+\epsilon'}$  for decay  $\overline{B}^0 \rightarrow \pi^+\pi^-$  in unit of percent.

	CLEO	BaBar	Belle
$\mathcal{A}_{CP}(\pi^\pm K^\mp)$	$-4 \pm 16$	$-7 \pm 8 \pm 2$	$4.4_{-16.7-2.1}^{+18.6+1.8}$
$\mathcal{A}_{CP}(\pi^0 K^\pm)$	$-29 \pm 23$	$0 \pm 18 \pm 4$	$-5.9_{-19.6-1.7}^{+22.2+5.5}$
$\mathcal{A}_{CP}(\pi^\pm K^0)$	$18 \pm 24$	$-21 \pm 18 \pm 3$	$9.8_{-34.3-6.3}^{+43.0+2.0}$
$\mathcal{A}_{CP}(K^\pm \eta')$	$3 \pm 12$		$6 \pm 15 \pm 1$
$a_{\epsilon'}(\pi^+\pi^-)$		$-25_{-47}^{+45} \pm 14$	
$a_{\epsilon+\epsilon'}(\pi^+\pi^-)$		$3_{-56}^{+53} \pm 11$	

TABLE VI. The dependence of time-integrated CP-violating asymmetries  $a_{\epsilon'}$ ,  $a_{\epsilon+\epsilon'}$ , and  $\mathcal{A}_{CP}$  (in units of percent) for  $\overline{B}^0(B^0) \rightarrow \pi^0\pi^0, \pi^0\eta^{(\prime)}, \eta^{(\prime)}\eta^{(\prime)}$  on renormalization scale  $\mu$ , with the default values of various parameters in the BBNS approach.

Decay Modes	scale $\mu$	$a_{\epsilon'}^f$	$a_{\epsilon'}^{f+a}$	$a_{\epsilon+\epsilon'}^f$	$a_{\epsilon+\epsilon'}^{f+a}$	$\mathcal{A}_{CP}^f$	$\mathcal{A}_{CP}^{f+a}$
$\overline{B}^0(B^0) \rightarrow \pi^0\pi^0$	$m_b/2$	-57.3	-69.3	-32.0	26.5	-52.6	-32.6
	$m_b$	-45.1	-79.0	-66.8	-12.4	-61.3	-57.4
	$2m_b$	-38.3	-82.4	-89.2	-46.3	-67.5	-75.8
$\overline{B}^0(B^0) \rightarrow \pi^0\eta$	$m_b/2$	35.5	62.7	9.72	-30.7	27.8	26.3
	$m_b$	31.5	63.3	12.2	-19.3	26.4	32.1
	$2m_b$	29.5	65.6	15.8	-9.75	26.8	38.1
$\overline{B}^0(B^0) \rightarrow \pi^0\eta'$	$m_b/2$	44.2	84.8	25.9	-35.3	41.2	38.5
	$m_b$	41.8	81.0	19.6	-28.2	36.6	39.4
	$2m_b$	37.1	79.3	18.3	-17.4	33.0	43.5
$\overline{B}^0(B^0) \rightarrow \eta\eta$	$m_b/2$	55.5	47.3	58.8	51.4	64.2	55.4
	$m_b$	43.1	36.4	71.1	69.9	61.9	57.0
	$2m_b$	34.7	26.6	82.6	84.4	62.0	57.6
$\overline{B}^0(B^0) \rightarrow \eta'\eta'$	$m_b/2$	30.7	76.8	95.2	52.7	65.4	75.2
	$m_b$	37.8	65.6	92.3	71.9	68.6	77.1
	$2m_b$	36.7	48.1	92.9	87.0	68.2	72.8
$\overline{B}^0(B^0) \rightarrow \eta\eta'$	$m_b/2$	55.6	49.5	74.1	77.8	71.5	69.3
	$m_b$	46.0	35.3	81.7	87.3	68.9	64.6
	$2m_b$	37.4	23.5	88.9	94.2	66.8	60.2

TABLE VII. CP-violating asymmetries  $a_{\epsilon'}$ (%) and  $a_{\epsilon+\epsilon'}$ (%) for neutral  $B$  meson decays with default values of various parameters using the BBNS approach.

Decay Modes	$\gamma = 60^\circ$				$\gamma = 90^\circ$				$\gamma = 120^\circ$			
	$a_{\epsilon'}^f$	$a_{\epsilon'}^{f+a}$	$a_{\epsilon+\epsilon'}^f$	$a_{\epsilon+\epsilon'}^{f+a}$	$a_{\epsilon'}^f$	$a_{\epsilon'}^{f+a}$	$a_{\epsilon+\epsilon'}^f$	$a_{\epsilon+\epsilon'}^{f+a}$	$a_{\epsilon'}^f$	$a_{\epsilon'}^{f+a}$	$a_{\epsilon+\epsilon'}^f$	$a_{\epsilon+\epsilon'}^{f+a}$
$\pi^+\pi^-$	4.17	11.5	55.1	54.8	5.85	16.1	-30.7	-30.6	6.64	17.7	-92.0	-91.1
$\pi^0\eta$	31.2	60.8	11.4	-21.1	25.0	43.5	7.27	-22.1	16.6	27.3	4.21	-16.0
$\pi^0\eta'$	41.6	77.4	18.4	-31.8	34.7	54.5	11.5	-35.8	23.5	34.0	6.54	-26.3
$\pi^0\pi^0$	-41.5	-76.6	-65.3	-16.0	-25.6	-56.9	-49.8	-23.7	-15.1	-36.4	-32.1	-18.8
$\eta\eta$	45.7	38.5	70.6	69.9	53.6	44.4	60.2	61.4	47.2	38.4	43.3	45.0
$\eta'\eta'$	41.7	70.3	89.7	68.4	65.7	86.9	65.3	42.9	89.9	81.1	38.4	21.0
$\eta\eta'$	49.7	38.4	81.0	87.4	65.5	53.4	68.8	80.5	66.1	58.0	50.7	65.7
$K_s^0\pi^0$	1.78	2.37	77.0	76.6	2.14	2.83	74.1	73.7	1.92	2.54	58.8	58.3
$K_s^0\eta$	3.08	3.62	77.8	77.4	3.72	4.36	75.1	74.7	3.38	3.95	59.9	59.3
$K_s^0\eta'$	-1.92	-2.20	73.9	74.3	-2.25	-2.58	70.3	70.8	-1.97	-2.26	54.7	55.2
$\overline{K}^0K^0$	21.0	20.8	9.08	3.74	16.6	16.1	6.30	2.16	10.9	10.5	3.86	1.17
$K^+K^-$	—	0	—	72.9	—	0	—	3.47	—	0	—	-68.0

TABLE VIII. CP-violating asymmetries  $\mathcal{A}_{CP}$ (%) for decays of  $B \rightarrow PP$  with default values of various parameters using the BBNS approach.

Decay modes	$\gamma = 60^\circ$		$\gamma = 90^\circ$		$\gamma = 120^\circ$	
	$\mathcal{A}_{CP}^f$	$\mathcal{A}_{CP}^{f+a}$	$\mathcal{A}_{CP}^f$	$\mathcal{A}_{CP}^{f+a}$	$\mathcal{A}_{CP}^f$	$\mathcal{A}_{CP}^{f+a}$
$\overline{B}^0(B^0) \rightarrow \pi^+\pi^-$	28.9	33.6	-10.8	-4.08	-39.6	-31.9
$B^\pm \rightarrow \pi^\pm\pi^0$	0.07	—	0.09	—	0.08	—
$B^\pm \rightarrow \pi^\pm\eta$	11.5	25.5	18.6	40.3	27.2	55.4
$B^\pm \rightarrow \pi^\pm\eta'$	5.08	19.3	7.55	28.1	9.16	32.9
$\overline{B}^0(B^0) \rightarrow \pi^0\eta$	25.8	29.7	19.8	17.9	12.8	10.2
$\overline{B}^0(B^0) \rightarrow \pi^0\eta'$	35.9	35.4	28.1	18.5	18.5	9.60
$\overline{B}^0(B^0) \rightarrow \pi^0\pi^0$	58.1	57.6	40.4	48.4	25.2	32.7
$\overline{B}^0(B^0) \rightarrow \eta\eta$	63.5	58.4	63.7	58.2	51.4	46.5
$\overline{B}^0(B^0) \rightarrow \eta'\eta'$	69.9	78.4	74.0	77.1	76.9	62.9
$\overline{B}^0(B^0) \rightarrow \eta\eta'$	71.0	66.7	75.5	73.2	67.3	69.2
$\overline{B}^0(B^0) \rightarrow K^\mp\pi^\pm$	-6.53	-16.1	-5.91	-14.8	-4.20	-10.7
$\overline{B}^0(B^0) \rightarrow K_S^0\pi^0$	37.8	38.0	36.7	36.9	29.3	29.4
$B^\mp \rightarrow K^\mp\pi^0$	-7.24	-15.0	-6.69	-14.1	-4.83	-10.3
$B^\mp \rightarrow K_S^0\pi^\mp$	-0.84	-1.05	-0.99	-1.24	-0.88	-1.10
$B^\mp \rightarrow K^\mp\eta$	8.35	14.0	12.8	21.1	16.3	26.3
$B^\mp \rightarrow K^\mp\eta'$	-3.19	-7.50	-3.41	-8.12	-2.75	-6.62
$\overline{B}^0(B^0) \rightarrow K_S^0\eta$	39.1	39.2	38.2	38.4	30.7	30.8
$\overline{B}^0(B^0) \rightarrow K_S^0\eta'$	34.0	33.9	32.0	32.0	24.8	24.8
$B^\mp \rightarrow K^\mp K_S^0$	21.0	26.4	16.6	20.2	10.9	13.1
$\overline{B}^0(B^0) \rightarrow \overline{K}^0K^0$	18.0	15.4	13.8	11.5	8.97	7.38
$\overline{B}^0(B^0) \rightarrow K^+K^-$	—	34.7	—	1.65	—	-32.4

TABLE IX. The dependence of CP-averaged branching ratio and CP asymmetries for  $B^\pm \rightarrow K^\pm \pi^0$  on  $\varrho$ ,  $\phi$  in endpoint divergence  $\int_0^1 dx/x$ .  $\text{BR}^f$  and  $\text{BR}^{f+a}$  have the same meanings as those in Table IV.  $\mathcal{A}_{CP}^f$  and  $\mathcal{A}_{CP}^{f+a}$  can be defined in a similar way. The results are calculated with default values of other parameters at  $\mu = m_b$  using the BBNS approach.

$\varrho$	0	3				6			
$\phi(\text{deg})$	0~360	0	90	180	270	0	90	180	270
$\text{BR}^f(10^{-6})$	6.37	6.31	6.36	6.43	6.38	6.25	6.35	6.49	6.39
$\text{BR}^{f+a}(10^{-6})$	7.51	11.8	6.75	6.43	6.18	21.3	4.63	7.89	3.48
$\mathcal{A}_{CP}^f(\%)$	8.28	8.45	7.15	8.11	9.40	8.63	6.02	7.94	10.5
$\mathcal{A}_{CP}^{f+a}(\%)$	7.24	5.15	14.2	8.11	1.47	3.32	29.5	6.81	-12.4

FIGURES

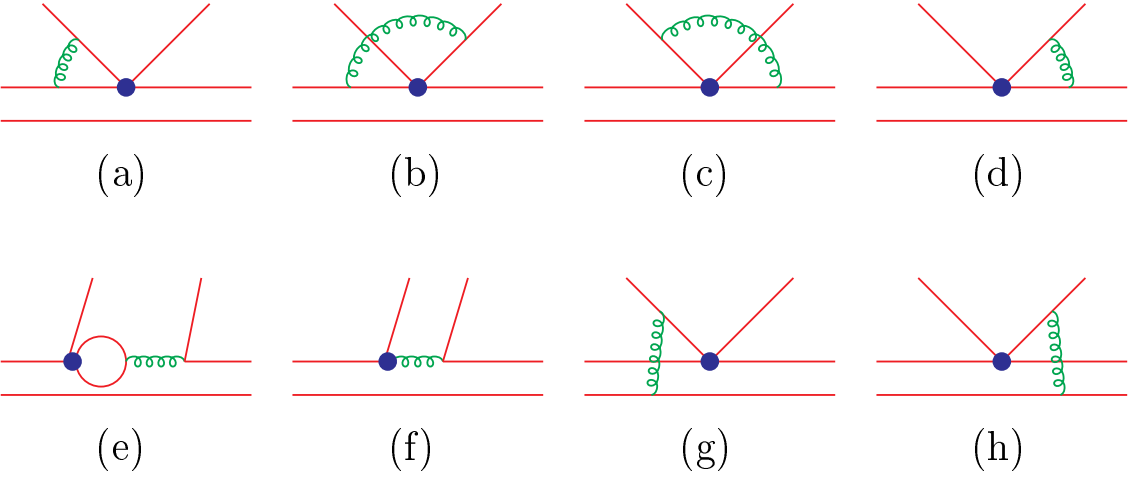


FIG. 1. Order of  $\alpha_s$  corrections to hard-scattering kernels. The upward quark lines represent the ejected light meson from  $b$  quark weak decays. These diagrams are commonly called vertex corrections, penguin corrections and hard spectator diagrams for Fig.(a)-(d), (e)-(f) and (g)-(h), respectively.

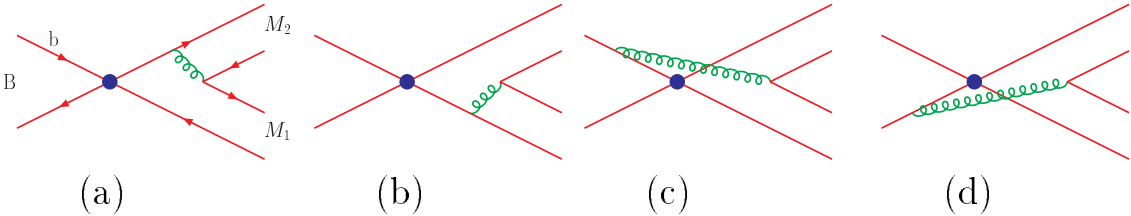


FIG. 2. Order of  $\alpha_s$  corrections to annihilation diagrams for  $B \rightarrow PP$

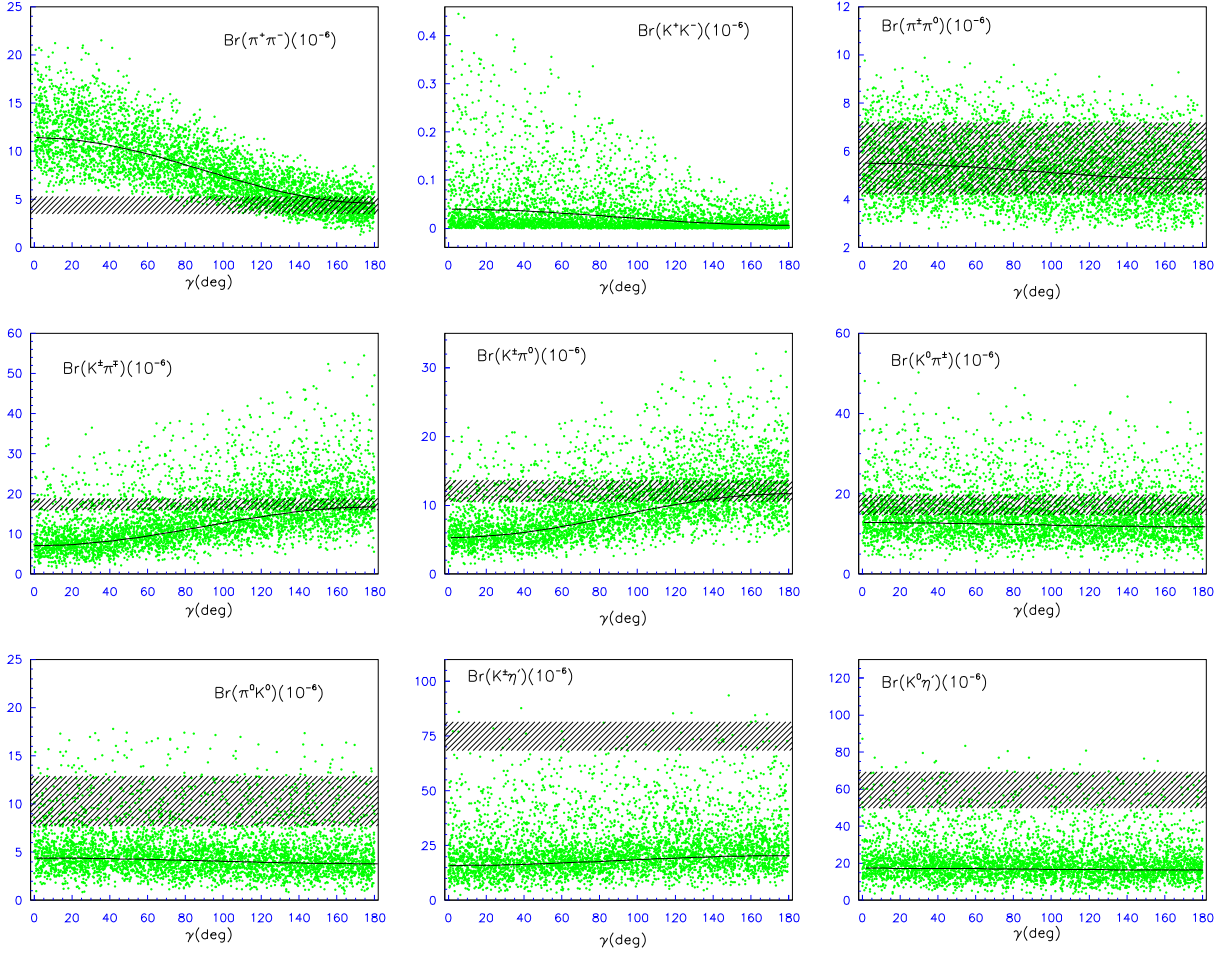


FIG. 3. CP-averaged branching ratios as functions of  $\gamma$ . The solid lines are drawn with the default values at the scale of  $\mu = m_b$ , the horizontal slashed-line bands correspond to experimental data within one standard error, and the dot-shades denote the variation of the theory input parameters, including the CKM elements, the form factors, the uncertainty from weak annihilation and hard spectator scattering.



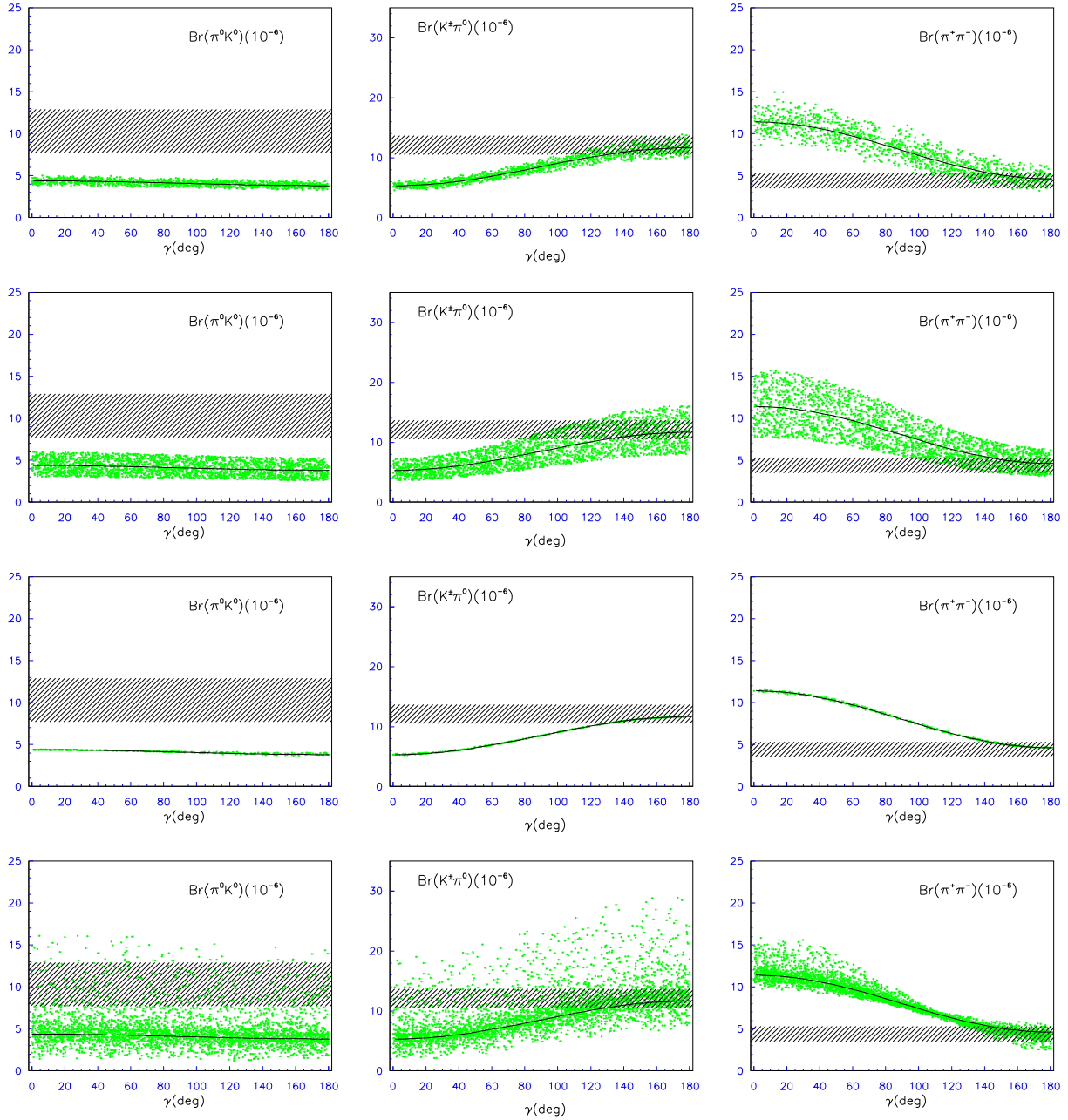


FIG. 4. The dependence of CP-averaged branching ratios for  $B^0 \rightarrow \pi^0 K^0$ ,  $B^\pm \rightarrow K^\pm \pi^0$  and  $B^0 \rightarrow \pi^+ \pi^-$  on the variations of input parameters under the QCDF approach at the renormalization scale  $\mu = m_b$ . The lines and bands have the same meaning as in Fig. 3, and the dot-shades correspond to the variation of the CKM matrix elements, in particular  $|V_{ub}|$  (the first row), form factors (the second row), endpoint divergences in the hard spectator scattering  $X_H$  (the third row) and weak annihilations  $X_A$  (the fourth row).

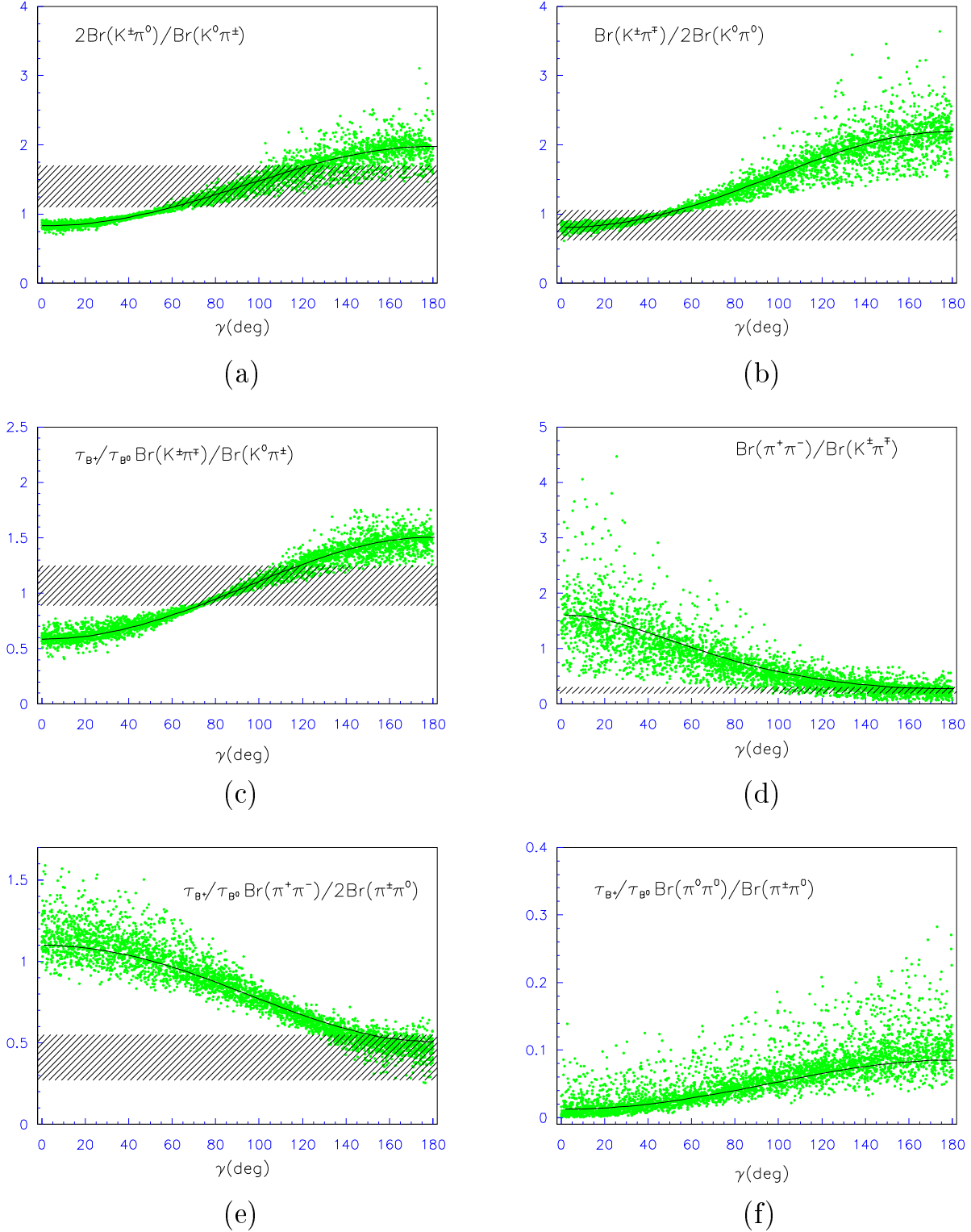


FIG. 5. Ratios of CP-averaged branching fractions versus  $\gamma$ . The lines, bands and dot-shades have the same meaning as in Fig. 3.